Synthesis and Reactivity of the Iridium Vinylidene $Ir{=}C{=}CH_2[N(SiMe_2CH_2PPh_2)_2]$. Formation of Carbon–Carbon Bonds via Migratory Insertion of a Vinylidene Unit

Michael D. Fryzuk,*,† Li Huang, Neil T. McManus, Patrick Paglia,‡ Steven J. Rettig,§ and Graham S. White∥

Department of Chemistry, University of British Columbia, 2036 Main Mall, Vancouver, BC, Canada V6T 1Z1

Received March 23, 1992

The synthesis of the 16-electron iridium vinylidene complex $Ir{=}C{=}CH_2[N(SiMe_2CH_2PPh_2)_2]$ is described by starting from the cyclooctene derivative $Ir(\eta^2\text{-}C_8H_{14})[N(SiMe_2CH_2PPh_2)_2]$ with addition of acetylene. This vinylidene complex reacts with a variety of electrophiles; thus, reaction with AlR_3 (R = Me, Et) or $GaMe_3$ leads to the formation of the new derivatives $Ir(ER_2)CR{=}CH_2[N(SiMe_2CH_2PPh_2)_2]$ (E = Al, R = Me, Et; E = Ga, R = Me). These complexes result from oxidative addition of the ER_3 reagent to the coordinatively unsaturated Ir(I) vinylidene followed by migratory insertion to generate the carbon–carbon bond of the substituted vinyl moiety. Oxidative addition of methyl iodide generates as the final product the allyl iodide derivative $Ir(\eta^3\text{-}C_3H_5)I[N(SiMe_2CH_2PPh_2)_2]$. This last transformation has been examined in detail using NMR spectroscopy to follow the course of the reaction. A number of intermediates could be observed: the first species is the oxidative adduct $Ir{=}C{=}CH_2(Me)I[N(SiMe_2CH_2PPh_2)_2]$, which undergoes migratory insertion to generate the isopropenyl iodide $Ir(CMe{=}CH_2)I[N(SiMe_2CH_2PPh_2)_2]$, which then rearranges to the allyl product. A third intermediate, believed to be an allene–amine derivative of the formula $Ir(\eta^2\text{-}H_2C{=}C{=}CH_2)I[HN(SiMe_2CH_2PPh_2)_2]$ is observed but was found not to be on the pathway to the allyl complex. Extension to other alkyl halides was attempted; reactions with ethyl iodide and benzyl bromide do proceed, but the resultant product mixtures are complex. Crystallographic data: $Ir{=}C{=}CH_2[N(SiMe_2CH_2PPh_2)_2]\cdot C_6H_5CH_3$, triclinic, a = 11.485 (3) Å, b = 115.498 (6) Å, c = 11.047 (5) Å, α = 92.00 (4)°, β = 103.31 (3)°, γ = 85.20 (3)°, Z = 2, space group $P\bar{1}$; $Ir(\eta^3\text{-}C_3H_5)I[N(SiMe_2CH_2PPh_2)_2]$, monoclinic, a = 9.571 (4) Å, b = 9.267 (6) Å, c = 39.262 (5) Å, β = 95.22 (3)°, Z = 4, space group $P2_1/n$; $Ir(AlMe_2)CMe{=}CH_2[N(SiMe_2CH_2PPh_2)_2]$, monoclinic, a = 18.823 (6) Å, b = 9.701 (2) Å, c = 21.359 (8) Å, β = 111.78 (2)°, Z = 4, space group $P2_1/c$; $Ir(GaMe_2)CMe{=}CH_2[N(SiMe_2CH_2PPh_2)_2]$, monoclinic, a = 18.816 (4) Å, b = 9.725 (3) Å, c = 21.4429 (4) Å, β = 111.58 (1)°, Z = 4, space group $P2_1/c$; $IrMeI_2[HN(SiMe_2CH_2PPh_2)_2]\cdot C_6H_6$, orthorhombic, a = 36.250 (5) Å, b = 11.368 (12) Å, c = 9.892 (8) Å, Z = 4, space group $Pna2_1$. The structures were all solved by heavy-atom methods and were refined by full-matrix least-squares procedures to R = 0.027, 0.026, 0.034, 0.034, and 0.032 for 7795, 5050, 5723, 7025, and 2806 reflections with $I \geq 3\sigma(I)$, respectively.

Introduction

The formation of carbon–carbon bonds via migratory insertion within the coordination sphere of a metal complex is a fundamental process in organometallic chemistry. While there are many variants and a host of different reaction partners that are included under the umbrella of migratory insertion reactions,[1] a relatively unstudied example is the combination of a hydrocarbyl and a metal–carbon double-bonded species as shown in Scheme I. Migratory insertion reactions involving metal complexes with carbene or alkylidene ligands (reaction a in Scheme I) have been invoked as key steps in Fischer–Tropsch mechanisms[2-4] and have been examined recently.[5-9] On the other hand, the corresponding transformations of vinylidene ligands are largely unknown, although there is some evidence that oligomerization of terminal alkynes may involve migratory insertion reactions of intermediate vinylidene complexes.[10] This is not because vinylidene-containing metal complexes are rare; on the contrary, the vinylidene unit is rather common across most of the transition series[11-16] and has been exploited in organic synthesis using transition-metal reagents.[17-19] However, what is difficult to find are metal complexes that contain both a vinylidene ligand and a hydrocarbyl unit, as is necessary for the migratory insertion reaction shown in (b) in Scheme I.[10,20,21]

Scheme I

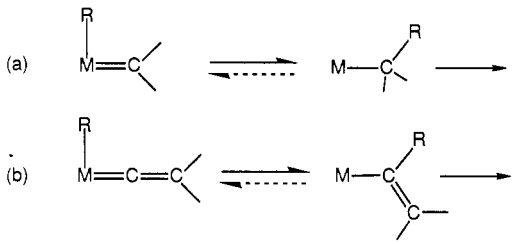

Our efforts in this area were spurred by the ability to prepare two simple iridium complexes containing metal–

† E. W. R. Steacie Fellow (1990–1992).

‡ Fonds National de la Recherche Scientifique (Suisse) Postdoctoral Fellow (1989–1991).

§ Professional Officer: UBC Crystallographic Service.

∥ NSERC Postdoctoral Fellow (1988–1990).

(1) Collman, J. P.; Hegedus, L. S.; Norton, J. R.; Finke, R. G. *Principles and Applications of Organotransition Metal Chemistry*; University Science Books: Mill Valley, CA, 1987.
(2) Brady, R. C., III; Pettit, R. *J. Am. Chem. Soc.* **1980**, *102*, 6181.
(3) Maitlis, P. M. *Pure Appl. Chem.* **1989**, *61*, 1747.
(4) Ma, F.; Sunley, G. J.; Saez, I. M.; Maitlis, P. M. *J. Chem. Soc., Chem. Commun.* **1990**, 1279.
(5) Thorn, D. L.; Tulip, T. H. *J. Am. Chem. Soc.* **1981**, *103*, 5984.
(6) Threlkel, R. S.; Bercaw, J. E. *J. Am. Chem. Soc.* **1981**, *103*, 2650.
(7) Kletzin, H.; Werner, H.; Serhadli, O.; Ziegler, M. L. *Angew. Chem., Int. Ed. Engl.* **1983**, *22*, 46.
(8) Jernakoff, P.; Cooper, N. J. *J. Am. Chem. Soc.* **1984**, *106*, 3026.
(9) Hoover, J. F.; Stryker, J. M. *J. Am. Chem. Soc.* **1990**, *112*, 464.
(10) Selnau, H. E.; Merola, J. S. *J. Am. Chem. Soc.* **1991**, *113*, 4008.
(11) Bruce, M. I.; Swincer, A. G. *Adv. Organomet. Chem.* **1983**, *22*, 59.
(12) Bruce, M. I.; Humphrey, M. G. *Aust. J. Chem.* **1989**, *42*, 1067.
(13) van Asselt, A.; Burger, B. J.; Gibson, V. C.; Bercaw, J. E. *J. Am. Chem. Soc.* **1986**, *108*, 5347.
(14) Werner, H.; Höhn, A.; Schulz, M. *J. Chem. Soc., Dalton Trans.* **1991**, 777.
(15) Birdwhistell, K. R.; Tonker, T. L.; Templeton, J. L. *J. Am. Chem. Soc.* **1985**, *107*, 4474.

0276-7333/92/2311-2979$03.00/0

carbon double bonds: the methylidene complex **1**[22] and the vinylidene derivative **2**.[23] Access to these very similar complexes should allow one to compare the relative reactivities of these two ligand types under the influence of identical ancillary ligands and the same metal center. In

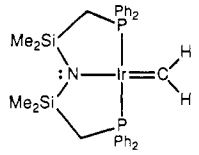

1

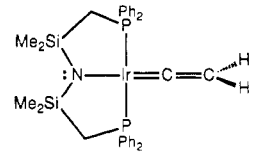

2

this paper we detail the preparation and reactivity of the vinylidene complex **2**, in particular, migratory insertion reactions with a variety of carbon-based electrophiles. Some of these results have been reported in preliminary form.[23] In a future publication we will provide full details of the chemistry of the methylidene derivative **1**. However, it should be noted that both complexes **1** and **2** are coordinatively unsaturated 16-electron species and can be considered formally as Ir(I) systems. This is in contrast with most other vinylidene complexes, which are typically 18-electron complexes. Indeed, there are only a handful of vinylidene complexes that are not coordinatively saturated; in addition to **2**, other related examples are the complexes *trans*-M=C=CHR(X)$(PPr^i_3)_2$ (M = Rh, Ir).[14,20,24,25] The fact that the vinylidene complex **2** both is coordinatively unsaturated and is in a low formal oxidation state should allow one to finesse systems with both a hydrocarbyl and a vinylidene unit intact (reaction b in Scheme I) via oxidative-addition reactions with carbon-based electrophiles. As is reported here, this was accomplished and has allowed for the first direct observation of the migratory insertion of a vinylidene and a metal alkyl species.

Experimental Section

General Procedures. All manipulations were performed under prepurified nitrogen in a Vacuum Atmospheres HE-553-2 workstation equipped with a MO-40-2H purification system or in Schlenk-type glassware. Toluene and hexanes were predried over CaH_2 and then deoxygenated by distillation from sodium–benzophenone ketyl and molten sodium, respectively, under argon. Tetrahydrofuran was predried by refluxing over CaH_2 and then distilled from sodium–benzophenone ketyl under argon. Deuterated benzene (C_6D_6, 99.6 atom % D) and deuterated toluene (C_7D_8, 99.6 atom % D), purchased from MSD Isotopes, were dried over activated 4-Å molecular sieves, vacuum-transferred, and freeze–pump–thawed three times before use. The complex Ir(η^2-C_8H_{14})[N($SiMe_2CH_2PPh_2$)$_2$] (**3**) was prepared according to the published procedure.[26]

The ^1H NMR spectra were recorded in C_6D_6 or $CD_3C_6D_5$ on a Varian XL-300 or a Bruker WH-400 spectrometer. With C_6D_6 as the solvent, the spectra were referenced to the residual solvent protons at 7.15 ppm; when $CD_3C_6D_5$ was used, the spectra were referenced to the CD_2H residual proton at 2.09 ppm. The $^{31}P\{^1H\}$ NMR spectra were recorded at 121.4 MHz on the Varian XL-300 instrument and were referenced to external $P(OMe)_3$ set at +141.00 ppm relative to 85% H_3PO_4. The $^{13}C\{^1H\}$ NMR and $^2H\{^1H\}$ NMR spectra were run in C_6D_6 at 75.4 and 46.0 MHz, respectively, on the Varian XL-300 spectrometer. The $^{13}C\{^1H\}$ NMR spectra were referenced at 128.00 ppm (triplet for the solvent), and the $^2H\{^1H\}$ spectra were referenced at 7.15 ppm, the residual solvent protons. Variable-temperature NMR spectral studies and various 1D- and 2D-NMR experiments (e.g. selective decoupling studies, APT and HETCOR experiments) were conducted on the Varian XL-300 spectrometer. Infrared spectra were recorded on a Pye-Unicam SP-1100 or a Nicolet 5DX Fourier transform spectrophotometer with the samples as KBr pellets or in solution between 0.1-mm NaCl plates. UV–vis spectra were recorded on a Perkin-Elmer 5523 UV–vis spectrophotometer stabilized at 20 °C. Carbon, hydrogen, and nitrogen analyses were performed by Mr. P. Borda of this department.

The electrophiles of CH_3I, CH_3CH_2I, and CD_3I (99.9 atom % D, purchased from MSD Isotopes) were dried over P_2O_5 and vacuum-transferred prior to use. The alkylaluminum reagents AlR_3 (R = Me, Et) were purchased from Aldrich and used as received; $GaMe_3$ was purchased from Strem.

Ir(η^2-C_2H_2)[N($SiMe_2CH_2PPh_2$)$_2$]. A solution of Ir(η^2-C_8H_{14})[N($SiMe_2CH_2PPh_2$)$_2$] (0.1 g, 0.12 mmol) in toluene (5 mL) was stirred at room temperature under 20-cm pressure of acetylene for 20 min, and then all of the volatiles were removed in vacuo. The residue was redissolved in the minimum amount of toluene and the solution then cooled at −30 °C to yield the product as orange, thermally labile crystals (0.03 g, 33%). ^1H NMR (δ, 300 MHz, C_6D_6): $SiMe_2$, 0.25 (s); PCH_2Si, 1.70 (vt, N = 3.6 Hz); HC≡CH, 2.45 (s); H_{arom}, 7.05 (m, para/meta); 7.70 (m, ortho).

Ir=C=CH_2[N($SiMe_2CH_2PPh_2$)$_2$]. A solution of Ir(η^2-C_8H_{14})[N($SiMe_2CH_2PPh_2$)$_2$] (0.1 g, 0.12 mmol) in toluene (5 mL) was stirred at room temperature under 20-cm pressure of acetylene for 20 min. The volatile materials were removed in vacuo, and the residue was redissolved in the minimum amount of toluene (5 mL). The orange solution was stirred overnight, yielding a deep red solution. After evaporation in vacuo, the resulting residue was extracted with hexanes and the solution filtered through Celite. Volatiles were removed, and the compound recrystallized from toluene at −30 °C to yield the vinylidene complex as red crystals (0.12 g, 66%). Anal. Calcd for $C_{32}H_{38}IrNP_2Si_2 \cdot C_7H_8$: C, 55.82; H, 5.53; N, 1.67. Found: C, 56.31; H, 5.44; N, 2.00 (the toluene of crystallization was confirmed by ^1H NMR spectroscopy). ^1H NMR (δ, 300 MHz, C_6D_6): =CH_2, −3.53 (t, $^4J_{PH}$ = 3.5 Hz); $SiMe_2$, 0.16 (s); PCH_2Si, 1.90 (vt, N = 5.3 Hz); H_{arom}, 7.08 (m, para/meta), 7.94 (m, ortho). $^{31}P\{^1H\}$ NMR (δ, 121.41 MHz, C_6D_6): 15.8 (s). ^{13}C NMR (δ, 75.4 MHz, C_6D_6): C_β, 91.6 (s); C_α, 268.1 (t, $^2J_{PC}$ = 7.0 Hz). IR (KBr): ν(C=C) 1648 cm^{-1}.

Ir($AlMe_2$)CMe=CH_2[N($SiMe_2CH_2PPh_2$)$_2$]. To a stirred solution of the vinylidene complex (75 mg, 0.1 mmol) at room temperature in toluene (1 mL) was added an excess (40 μL, 3 equiv) of 2 M $AlMe_3$ (Aldrich) solution. The color immediately turned to bright lemon. Stirring was continued for 15 min, during which time crystals separated from solution: 30 mg (37%). Anal. Calcd for $C_{35}H_{47}AlNP_2Si_2Ir$: C, 51.32; H, 5.78; N, 1.71. Found: C, 51.45; H, 5.84; N, 1.73. ^1H NMR (δ, 300 MHz, C_6D_6): $SiMe_2$, −0.05 (s), 0.40 (s); $AlMe_2$, −0.03 (s); PCH_2Si, 1.91 (dvt, J_{gem} = 14.3, N = 5.2 Hz) and 2.53 (dvt, N = 5.3 Hz); C(Me)=C, 1.92 (s); =CH_2, 4.77 (s) and 6.01 (s); H_{arom}, 7.20 (m, para/meta), 7.92 and 8.03 (m, ortho). $^{31}P\{^1H\}$ NMR (δ, 121.4 MHz, C_6D_6): 18.0 (s). IR (KBr): ν(C=C) 1590 cm^{-1}.

Ir($AlEt_2$)CEt=CH_2[N($SiMe_2CH_2PPh_2$)$_2$]. The same procedure as used above for $AlMe_3$ was followed except that $AlEt_3$ was used. Anal. Calcd for $C_{38}H_{53}AlNP_2Si_2Ir$: C, 53.00; H, 6.20; N, 1.63. Found: C, 52.27; H, 6.20; N, 1.64. ^1H NMR (δ, 300 MHz, C_6D_6): $SiMe_2$, 0.06 (s) and 0.48 (s); PCH_2Si, 1.88 (dvt, J_{gem} = 14.4,

(16) Senn, D. R.; Wong, A.; Patton, A. T.; Marsi, M.; Strouse, C. E.; Gladysz, J. A. *J. Am. Chem. Soc.* **1988**, *110*, 6096.
(17) Landon, S. J.; Shulman, P. M.; Geoffroy, G. L. *J. Am. Chem. Soc.* **1985**, *107*, 6739.
(18) Liebeskind, L. S.; Chidambaram, R. *J. Am. Chem. Soc.* **1987**, *109*, 5025.
(19) Trost, B. M.; Dyker, G.; Kulawiec, R. J. *J. Am. Chem. Soc.* **1990**, *112*, 7809.
(20) Höhn, A.; Werner, H. *J. Organomet. Chem.* **1990**, *382*, 255.
(21) Beevor, R. G.; Freeman, M. J.; Green, M.; Morton, C. E.; Orpen, A. G. *J. Chem. Soc., Chem. Commun.* **1985**, 68.
(22) Fryzuk, M. D.; MacNeil, P. A.; Rettig, S. J. *J. Am. Chem. Soc.* **1985**, *107*, 6708–6710.
(23) Fryzuk, M. D.; McManus, N. T.; Rettig, S. J.; White, G. S. *Angew. Chem., Int. Ed. Engl.* **1990**, *29*, 73–75.
(24) Alonso, F. J. G.; Höhn, A.; Wolf, J.; Otto, H.; Werner, H. *Angew. Chem., Int. Ed. Engl.* **1985**, *24*, 406.
(25) Höhn, A.; Otto, H.; Dziallas, M.; Werner, H. *J. Chem. Soc., Chem. Commun.* **1987**, 852.
(26) Fryzuk, M. D.; MacNeil, P. A.; Rettig, S. J. *Organometallics* **1986**, *5*, 2469.

N = 5.1 Hz) and 2.53 (dvt, N = 5.3 Hz); $AlCH_2CH_3$, 0.61 (m); $AlCH_2CH_3$, 1.46 (t, J = 8.1 Hz); $C(CH_2CH_3)$=C, 2.19 (q, J = 7.4 Hz); CH_2CH_3, 0.98 (t, J = 7.4 Hz); =CH_2, 4.84 (br s) and 5.96 (br s); H_{arom}, 7.18 (m, meta/para), 7.85 and 7.98 (m, ortho). $^{31}P\{^1H\}$ NMR (δ, 121.4 MHz, C_6D_6): 17.7 (s). IR (KBr): ν(C=C) 1586 cm^{-1}.

Ir(GaMe$_2$)CMe=CH$_2$[N(SiMe$_2$CH$_2$PPh$_2$)$_2$]. The same procedure as used above for $AlMe_3$ was followed except that $GaMe_3$ was used. Recrystallization of the crude material from toluene–hexane gave yellow crystals in 55% yield. Anal. Calcd for $C_{35}H_{47}GaNP_2Si_2Ir \cdot {}^1/_2C_6H_{14}$: C, 50.44; H, 6.01; N, 1.55. Found: C, 50.59; H, 5.81; N, 1.70 (the 0.5 hexane of crystallization was confirmed by ^1H NMR spectroscopy). ^1H NMR (δ, 300 MHz, C_6D_6): $SiMe_2$ –0.06 (s), 0.39 (s); $GaMe_2$ –0.04 (s); C(Me)=C, 1.90 (s); PCH_2Si, 1.80 (dvt, J_{gem} = 14.3 Hz, N = 5.2 Hz); 2.36 (dvt, N = 5.2 Hz); =CH_2, 4.62 (s), 5.95 (s); H_{arom}, 7.10 (m, meta/para), 7.76 and 7.92 (m, ortho). $^{31}P\{^1H\}$ NMR (δ, 121.4 MHz, C_6D_6): 18.1 (s).

Ir(η^3-C$_3$H$_5$)I[N(SiMe$_2$CH$_2$PPh$_2$)$_2$]. Methyl iodide (excess) was condensed into a red solution of Ir=C=CH_2[N(SiMe$_2$CH$_2$PPh$_2$)$_2$] (80 mg, 0.12 mmol) in toluene (5 mL). The reaction mixture was stirred at room temperature until the solution turned yellow (ca. 1.5 h). All volatile materials were removed in vacuo, and the residue was redissolved in toluene (5 mL) and then stirred for an additional 48 h at room temperature. The initially yellow solution changed to green and returned to yellow, indicating completion of the reaction. The resulting solution was then concentrated and stored at –30 °C to give 70 mg (66%) of yellow crystals. Anal. Calcd for $C_{33}H_{41}IIrNP_2Si_2$: C, 44.59; H, 4.65; N, 1.58. Found: C, 44.90; H, 4.77; N, 1.46. ^1H NMR (δ, 300 MHz, C_6D_6): $SiMe_2$, 0.63 (s), 0.44 (s), 0.22 (s), 1.09 (s); PCH_2Si, 1.69 (m), 2.77 (m); H_{anti}, 0.80 (t), 1.58 (m); H_{syn}, 2.17 (t), 3.42 (m); $H_{central}$, 3.98 (m); H_{arom}, 6.94–7.69 (m, para/meta), 8.31 (m, ortho). $^{31}P\{^1H\}$ NMR (δ, 121.4 MHz, C_6D_6): PPh_2, –11.50 (d, $^2J_{PP}$ = 425 Hz); PPh_2, –4.22. $^{13}C\{^1H\}$ NMR (δ, 75 MHz, C_6D_6): Ir(η^3-H_2CCHCH_2), 29.4, 39.2 ($^1J_{C,H}$ = 156 Hz).

Ir(η^3-C$_3$H$_2$D$_3$)I[N(SiMe$_2$CH$_2$PPh$_2$)$_2$]. The procedure is analogous to that for the undeuterated material. Use of CD_3I (99.8% D) resulted in the product formation after 96 h. Anal. Calcd for $C_{33}H_{38}D_3IIrNP_2Si_2$: C, 44.44; H + D, 4.97; N, 1.57. Found: C, 44.80; H, 4.59; N, 1.62. ^1H NMR (δ, 300 MHz, C_6D_6): $SiMe_2$, 0.36 (s), 0.40 (s), 0.60 (s), 1.07 (s), PCH_2Si, 1.62 (m), 2.12 (m); H_{anti}, 0.74 (m), 1.54 (m); H_{syn}, 2.70 (m), 3.37 (m); PPh_2, H_{arom}, 6.90–7.60 (m, para/meta), 8.26 (m, ortho). $^{31}P\{^1H\}$ NMR (δ, 121.4 MHz, C_6D_6): PPh_2, –11.50 (d, $^2J_{P,P}$ = 424.30 Hz); PPh_2, –4.35 (d of br d, J = 12.1 Hz).

Ir(η^3-C$_3$H$_4$(CH$_3$))Br[N(SiMe$_2$CH$_2$PPh$_2$)$_2$]. Into a solution of Ir(η^2-C_8H_{14})[N(SiMe$_2$CH$_2$PPh$_2$)$_2$] (104 mg, 0.125 mmol) in toluene (5 mL) at –20 °C was syringed dropwise crotyl bromide (0.100 mL, 0.97 mmol). The temperature was allowed to rise, and the solution turned gradually pale green and finally lemon yellow within 30 min. The volatiles were removed in vacuo to generate the product as yellow crystals in virtually quantitative yield. Anal. Calcd for $C_{34}H_{43}BrIrNP_2Si_2 \cdot {}^1/_2C_7H_8$: C, 49.93; H, 5.25; N, 1.55. Found: C, 50.06; H, 5.33; N, 1.50 (the 0.5 toluene of crystallization was confirmed by ^1H NMR spectroscopy). ^1H NMR (δ, 300 MHz, C_6D_6): $SiMe_2$, 0.11 (s), 0.38 (s), 0.49 (s), 1.00 (s); H_{anti}, 0.64 (m), 2.21 (m); H_{syn}, 2.81 (m, $^3J_{central}$ = 7.5 Hz); $H_{central}$, 3.77 (ddd, $^3J_{anti}$ = 7.5 Hz); PCH_2Si, 1.43 (dd, J_{gem} = 12.5 Hz), 1.68 (m), 3.43 (m, J_P = 3.6 Hz, $J_{P'}$ = 9.0 Hz); CH_3, 0.80 (d, ^2J = 6.2 Hz); H_{arom}, 8.30 (m, ortho), 7.82 (m, ortho), 6.85–7.40 (m, meta/para). $^{31}P\{^1H\}$ NMR (δ, 121.4 MHz, C_6D_6): PPh_2, –10.40 (d, $^2J_{P,P}$ = 427 Hz); –4.45 (d).

IrMeI$_2$[HN(SiMe$_2$CH$_2$PPh$_2$)$_2$]. To a solution of the vinylidene complex (80 mg, 0.12 mmol) in toluene (5 mL) was vacuum-transferred an excess of methyl iodide (approximately 25 equiv). The reaction mixture was stirred for several days, during which time 100 mg (85%) of yellow crystals precipitated directly from solution. Anal. Calcd for $C_{31}H_{39}I_2NP_2Si_2Ir$: C, 37.58; H, 4.07; N, 1.41. Found: C, 38.02; H, 4.27; N, 1.37. ^1H NMR (δ, 300 MHz, C_6D_6/C_5D_5N): $SiMe_2$, 0.05 (s), 0.25 (s); CH_3Ir, 1.35 (m); $SiCH_2P$, 2.45 (m); NH, 3.80 (br, s); H_{arom}, 7.55 (m, para/meta), 8.55 (m, ortho). $^{31}P\{^1H\}$ NMR (δ, 121.4 MHz, C_6D_6/C_5D_5N): –21.7 (s).

Reaction of Ir=C=CH$_2$[N(SiMe$_2$CH$_2$PPh$_2$)$_2$] with Methyl Iodide. To a bright red solution of vinylidene complex **2** (40 mg, 0.054 mmol) in C_7D_8 (0.5 mL) in a sealable NMR tube was added CH_3I (7.0 μL, 0.112 mmol) at –30 °C. The solution was sealed, maintained at –30 °C, and quickly transferred to the NMR spectrometer with a probe temperature of –30 °C and was then monitored by $^{31}P\{^1H\}$, ^1H and $^{13}C\{^1H\}$ NMR spectroscopy.

At this temperature only Ir=C=CH_2(CH_3)I[N(SiMe$_2$CH$_2$PPh$_2$)$_2$] (**9**) is present by $^{31}P\{^1H\}$ NMR spectroscopy (singlet at –4.51 ppm). As the solution warms to room temperature, two additional signals are observed in the first 15 min: the isopropenyl intermediate Ir(CMe=CH_2)I[N(SiMe$_2$CH$_2$PPh$_2$)$_2$] (**10**) at 8.40 ppm (s) in ca. 15% yield and the allene–amine derivative species Ir(η^2-H_2C=C=CH_2)I[HN(SiMe$_2$CH$_2$PPh$_2$)$_2$] (**11**) at –10.12 ppm (s), but just in a trace amount. If the reaction is done in C_6D_6 at room temperature instead of at –30 °C in C_7D_8, within 15 min there are appreciable amounts of the isopropenyl complex **10** present and the allene–amine derivative **11** as well. The methyl–iodide adduct **9** disappears in approximately 6 h. The isopropenyl–iodide complex **10** increases to ca. 60% yield in the first 2 h and then it decreases slowly over a period of 48 h. The last detectable intermediate, the allene–amine derivative **11**, reaches its highest concentration (20%) in 4 h and decreases very slowly. Similar to complex **10**, **11** did not disappear until the end of the reaction. The allyl iodide product **8** is initially observed after approximately 2 h and increases to ca. 70% in 8 h and ca. 100% in 48 h.

All of the intermediates **9**–**11** in the reaction of vinylidene complex **2** with CH_3I could be identified by ^1H NMR and also by ^{13}C NMR spectroscopy with ^1H gated decoupling using $^{13}CH_3I$ instead of $^{12}CH_3I$.

Ir=C=CH$_2$(CH$_3$)I[N(SiMe$_2$CH$_2$PPh$_2$)$_2$] (9). ^1H NMR (δ, 300 MHz, C_6D_6): CH_3, 1.92 (t, $^3J_{PH}$ = 7 Hz); =CH_2, 5.10 (s), 5.45 (s); $SiMe_2$, –0.03 (s), 0.47 (s); PCH_2Si, 1.78 (dt, N = 5.4 Hz, J_{gem} = 14.4 Hz), 1.88 (dt, N = 5.4 Hz); PPh_2, 7.0–8.5 (m, obscured by aromatic protons in other complexes). $^{31}P\{^1H\}$ NMR (δ, 121.4 MHz, C_6D_6): –4.51 (s). $^{13}C\{^1H\}$ NMR (δ, 75.4 MHz, C_6D_6): IrMe, –28.7 (q, $^1J_{CH}$ = 130 Hz).

Ir(CMe=CH$_2$)I[N(SiMe$_2$CH$_2$PPh$_2$)$_2$] (10). ^1H NMR (δ, 300 MHz, C_6D_6): CH_3, 1.10 (s); =CH_2, 3.88 (s), 4.72 (s); $SiMe_2$, –0.24 (s), 0.49 (s); PCH_2Si, 1.54 (dt, N = 5.7 Hz, J_{gem} = 13.2 Hz), 2.13 (dt, N = 5.7 Hz); PPh_2, 7.0–8.5 (m, obscured by aromatic protons in other complexes). $^{31}P\{^1H\}$ NMR (δ, 121.4 MHz, C_6D_6): 8.40 (s). $^{13}C\{^1H\}$ NMR (δ, 75.4 MHz, C_6D_6): CH_3, 44.4 (q, $^1J_{CH}$ = 127 Hz).

Ir(η^2-H$_2$C=C=CH$_2$)I[HN(SiMe$_2$CH$_2$PPh$_2$)$_2$] (11). ^1H NMR (δ, 300 MHz, C_6D_6): η^2-H_2C=C, 1.60 (s); C=CH_2, 6.06 (s); $SiMe_2$, 0.11 (s), 0.16 (s); PCH_2Si, 2.24 (m); PPh_2, 7.0–8.5 (m, obscured by aromatic protons in other complexes). $^{31}P\{^1H\}$ NMR (δ, 121.4 MHz, C_6D_6): –10.12 (s). $^{13}C\{^1H\}$ NMR (δ, 75.4 MHz, C_6D_6): –CH_2, –0.20 (t, $^1J_{CH}$ = 155 Hz).

If CD_3I was used instead of CH_3I, the signal for the Ir–methyl protons (1.92 ppm, t, $^3J_{PH}$ = 7 Hz) for complex **9** did not appear and, in addition, the signals for the methyl protons in the isopropenyl group (1.10 ppm, s) for **10** and the methylene protons in the allene group (1.60 ppm, s) for **11** were not observed.

IrNCCH$_3$(CMe=CH$_2$)I[N(SiMe$_2$CH$_2$PPh$_2$)$_2$]. To a solution of Ir=C=CH_2[N(SiMe$_2$CH$_2$PPh$_2$)$_2$] (50 mg, 0.07 mmol) in toluene (1 mL) was added 1 equiv of CH_3I (5 μL) at room temperature. After the mixture was stirred for 3 h, 3 equiv of MeCN (5 μL) was added to the green solution and the color immediately turned to yellow. Although the $^{31}P\{^1H\}$ NMR spectrum indicated that complex **13** was formed in a virtually quantitative yield, only 21 mg of orange crystals was isolated from the reaction solution directly after 2 days at room temperature (33%). Anal. Calcd for $C_{35}H_{44}N_2IIrP_2Si_2$: C, 45.20; H, 4.77; N, 3.01. Found: C, 45.03; H, 4.83; N, 2.97. ^1H NMR (δ, 300 MHz, C_6D_6): $NCCH_3$, 2.1 (s); CCH_3, 1.38 (s); =CH_2, 5.48 (br, s); 5.96 (m); $SiMe_2$, –0.36 (s), 0.67 (s); PCH_2Si, 1.69 (dt, N = 5.7 Hz, J_{gem} = 13.2 Hz), 2.56 (dt, N = 6.6 Hz); H_{arom}, 7.1 (m, para/meta), 7.91, 8.47 (m, ortho). $^{13}P\{^1H\}$ NMR (δ, 121.4 MHz, C_6D_6): –21.5 (s).

X-ray Crystallographic Analyses. Crystallographic data for Ir=C=CH_2[N(SiMe$_2$CH$_2$PPh$_2$)$_2$]·$C_6H_5CH_3$, Ir(η^3-C_3H_5)I[N(SiMe$_2$CH$_2$PPh$_2$)$_2$], Ir(AlMe$_2$)CMe=CH_2[N(SiMe$_2$CH$_2$PPh$_2$)$_2$], Ir(GaMe$_2$)CMe=CH_2[N(SiMe$_2$CH$_2$PPh$_2$)$_2$], and IrMeI$_2$[HN(SiMe$_2$CH$_2$PPh$_2$)$_2$]·C_6H_6 appear in Table I. The final unit-cell parameters were obtained by least squares on the setting angles for 25 reflections with 2θ = 29.6–35.1, 27.3–35.0, 44.6–47.2,

Table I. Crystallographic Data[a,b]

compd	Ir=C=CH$_2$[PNP][c]	Ir(η^3-C$_3$H$_5$)I[PNP]	Ir(AlMe$_2$)CMe=CH$_2$[PNP]	Ir(GaMe$_2$)CMe=CH$_2$[PNP]	IrMeI$_2$[HPNP][d]
formula	$C_{39}H_{46}IrNP_2Si_2$	$C_{33}H_{41}IIrNP_2Si_2$	$C_{35}H_{47}AlIrNP_2Si_2$	$C_{35}H_{47}GaIrNP_2Si_2$	$C_{37}H_{46}I_2IrNP_2Si_2$
fw	839.14	888.94	819.08	861.82	1068.92
cryst syst	triclinic	monoclinic	monoclinic	monoclinic	orthorhombic
space group	$P\bar{1}$	$P2_1/n$	$P2_1/c$	$P2_1/c$	$Pna2_1$
a, Å	11.485 (3)	9.571 (4)	18.823 (6)	18.816 (4)	36.250 (5)
b, Å	15.498 (6)	9.267 (6)	9.701 (2)	9.725 (3)	11.368 (12)
c, Å	11.047 (5)	39.262 (5)	21.359 (8)	21.442 (4)	9.892 (8)
α, deg	92.00 (4)				
β, deg	103.31 (3)	95.22 (3)	111.78 (2)	111.58 (1)	
γ, deg	85.20 (3)				
V, Å^3	1907 (1)	3468 (4)	3622 (2)	3649 (2)	4077 (7)
Z	2	4	4	4	4
ρ_{calc}, g/cm^3	1.46	1.70	1.50	1.57	1.74
$F(000)$	844	1736	1648	1720	2064
μ(Mo Kα), cm^{-1}	36.59	48.99	38.73	45.42	49.23
cryst size, mm	0.15 × 0.30 × 0.40	0.15 × 0.15 × 0.25	0.10 × 0.25 × 0.35	0.20 × 0.35 × 0.50	0.15 × 0.15 × 0.30
transmissn factors	0.63–1.00	0.84–1.00	0.65–1.00	0.56–1.00	0.81–1.00
scan type	ω–2θ	ω	ω–2θ	ω–2θ	ω
scan range, deg in ω	1.10 + 0.35 tan θ	0.79 + 0.35 tan θ	1.21 + 0.30 tan θ	1.05 + 0.35 tan θ	1.04 + 0.35 tan θ
scan rate, deg/min	16	16	16	16	16
data collected	$+h,\pm k,\pm l$	$+h,+k,\pm l$	$+h,+k,\pm l$	$\pm h,+k,+l$	$+h,+k,\pm l$
$2\theta_{max}$, deg	60	55	55	65	55
cryst decay	negligible	negligible	negligible	negligible	4.3%
p factor in $\sigma(I)$ calcn	0.04	0.03	0.04	0.03	0.03
total no. of rflns	11671	9168	8600	13493	5265
no. of unique rflns	11122	8461	8352	13166	5265
R_{merge}	0.032	0.035	0.027	0.040	
no. of rflns with $I \geq 3\sigma(I)$	7795	5050	5723	7025	2806
no. of variables	415	361	379	380	405
R	0.027	0.026	0.034	0.034	0.032
R_w	0.032	0.030	0.040	0.035	0.032
GOF	1.04	1.17	1.41	1.24	1.13
max Δ/σ (final cycle)	0.02	0.07	0.04	0.004	0.06
residual density, e/Å^3	−0.60 to +0.83	−0.67 to +0.66	−3.00 to +1.85 (near Ir)	−0.86 to +1.45	−0.67 to +0.71

[a] The temperature was 294 K; the function minimized was $\sum w(|F_o| - |F_c|)^2$, where $w = 4F_o^2/\sigma^2(F_o^2)$, $R = \sum||F_o| - |F_c||/\sum|F_o|$, $R_w = (\sum w(|F_o| - |F_c|)^2/\sum w|F_o|^2)^{1/2}$, and GOF = $[\sum(|F_o| - |F_c|)^2/(m - n)]^{1/2}$. Values given for R, R_w, and GOF are based on those reflections with $I \geq 3\sigma(I)$. Data collection conditions: Rigaku AFC6S diffractometer, Mo Kα radiation (λ = 0.71069 Å), graphite monochromator, takeoff angle 6.0°, aperture 6.0 × 6.0 mm at a distance of 285 mm from the crystal, stationary background counts at each end of the scan (scan/background time ratio 2:1, up to 8 rescans), $\sigma^2(F^2) = [S^2(C + 4B) + (pF^2)^2]/Lp^2$ (S = scan rate, C = scan count, B = normalized background count). [b] [PNP] = [N(SiMe$_2$CH$_2$PPh$_2$)$_2$]; [HPNP] = [HN(SiMe$_2$CH$_2$PPh$_2$)$_2$]. [c] Crystallizes as a 1:1 toluene solvate. [d] Crystallizes as a 1:1 benzene solvate.

28.7–35.2, and 20.1–36.1° for the five complexes, respectively. The intensities of three standard reflections, measured every 150 reflections throughout the data collections, decayed uniformly by 4.3% for IrMeI$_2$[HN(SiMe$_2$CH$_2$PPh$_2$)$_2$]·C$_6$H$_6$ and remained constant for the other four compounds. The data were processed[27] and corrected for Lorentz and polarization effects, decay (where appropriate), and absorption (empirical, based on azimuthal scans for four reflections).

The structure analysis of Ir=C=CH$_2$[N(SiMe$_2$CH$_2$PPh$_2$)$_2$]·C$_6$H$_5$CH$_3$ was initiated in the centrosymmetric space group $P\bar{1}$ and that of IrMeI$_2$[HN(SiMe$_2$CH$_2$PPh$_2$)$_2$]·C$_6$H$_6$ in the noncentrosymmetric space group $Pna2_1$. These choices were based on the E statistics and the Patterson functions and were confirmed by the subsequent successful solutions and refinements of the structures. The structures were solved by heavy-atom methods, the coordinates of the heavy atoms being determined from the Patterson functions and those of the remaining non-hydrogen atoms from subsequent difference Fourier syntheses. The structure analysis of Ir(GaMe$_2$)CMe=CH$_2$[N(SiMe$_2$CH$_2$PPh$_2$)$_2$] was initiated with the coordinates of the isomorphous and isostructural aluminum analogue. All non-hydrogen atoms were refined with anisotropic thermal parameters. The hydrogen atoms of the vinylidene ligand in Ir=C=CH$_2$[N(SiMe$_2$CH$_2$PPh$_2$)$_2$]·C$_6$H$_5$CH$_3$ were refined with isotropic thermal parameters, and all other hydrogen atoms were fixed in idealized positions (N–H/C–H = 0.98 Å, $B_H = 1.2B_{bonded\ atom}$); the methylene hydrogen positions of the vinylidene unit were based on observed positions. Corrections for secondary extinction were applied for Ir=C=CH$_2$[N(SiMe$_2$CH$_2$PPh$_2$)$_2$]·C$_6$H$_5$CH$_3$ and Ir(GaMe$_2$)CMe=CH$_2$[N(SiMe$_2$CH$_2$PPh$_2$)$_2$], the final values of the extinction coefficients being 1.25 × 10^{-5} and 2.40 × 10^{-5}, respectively. Neutral atom scattering factors for all atoms and anomalous dispersion corrections for the non-hydrogen atoms were taken from ref 28. A parallel refinement of the structure of IrMeI$_2$[HN(SiMe$_2$CH$_2$PPh$_2$)$_2$]·C$_6$H$_6$ having the opposite polarity resulted in substantially higher residuals. Final atomic coordinates and equivalent isotropic thermal parameters, selected bond lengths, and selected bond angles appear in Tables II–IV, respectively (except for those of IrMeI$_2$[HN(SiMe$_2$CH$_2$PPh$_2$)$_2$]·C$_6$H$_6$, which are included as supplementary material). Hydrogen atom parameters, anisotropic thermal parameters, complete tables of bond lengths and bond angles, torsion angles, intermolecular contacts, and least-squares planes are included as supplementary material.

Scheme II

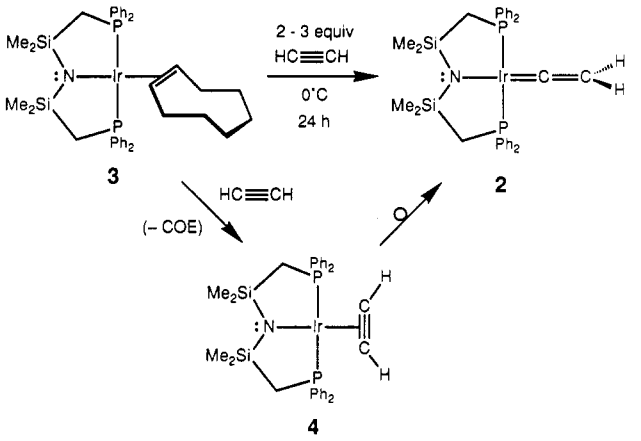

(27) TEXSAN/TEXRAY Structure Analysis Package, Molecular Structure Corp., 1985.

(28) *International Tables for X-Ray Crystallography*; Kynoch Press: Birmingham, U.K. (present distributor D. Reidel, Dordrecht, The Netherlands), 1974; Vol. IV, pp 99–102, 149.

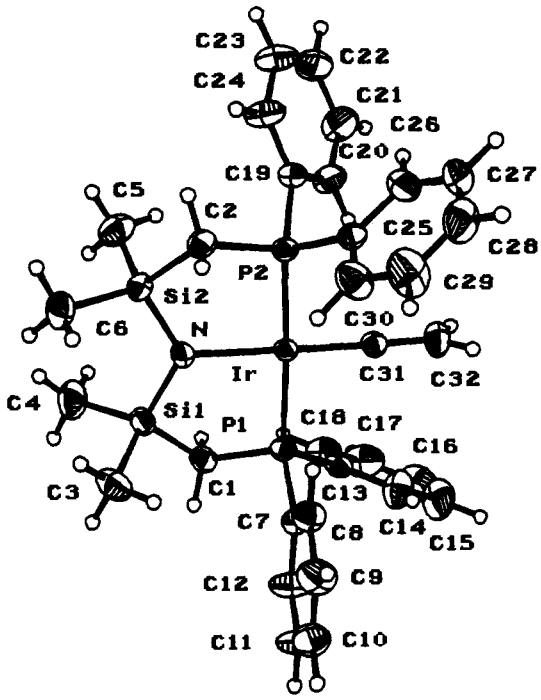

Figure 1. Molecular structure and numbering scheme for Ir=C=CH_2[$N(SiMe_2CH_2PPh_2)_2$] (2).

Results and Discussion

Synthesis and Structure of Ir=C=CH_2[$N(SiMe_2CH_2PPh_2)_2$]. The red-orange iridium vinylidene complex Ir=C=CH_2[$N(SiMe_2CH_2PPh_2)_2$ (2) is prepared by the addition of acetylene to the cyclooctene derivative Ir(η^2-C_8H_{14})[$N(SiMe_2CH_2PPh_2)_2$] (3)[26] by way of the transient Ir(η^2-C_2H_2)[$N(SiMe_2CH_2PPh_2)_2$] (4); this η^2-acetylene adduct 4 was only spectroscopically characterized because of its thermal lability (Scheme II). The transformation of 4 to the vinylidene 2 occurs over a period of 24 h in benzene or toluene without the observation of any intermediates (by ^1H NMR spectroscopy). Diagnostic of the vinylidene complex is the presence of an upfield triplet at −3.53 ppm ($^4J_{PH}$ = 3.5 Hz) for the Ir=C=CH_2 unit, in accord with other related iridium vinylidene complexes.[14,24,25]

The X-ray structure of the vinylidene complex is shown in Figure 1. The molecule shows a square-planar geometry about the iridium with the plane defined by the vinylidene unit (C=CH_2) very nearly perpendicular (dihedral angle of 98.64°) to this square plane. The iridium–disilylamide unit (Ir–NSi_2) is also planar (sum of the angles is 359.9°) and coplanar (dihedral angle of 177.3°) with the square plane of the complex. The iridium–carbon bond length (Ir–C(31)) of 1.806 (4) Å is rather short by comparison to the related distance of 1.868 (9) Å found in the methylidene complex Ir=CH_2[$N(SiMe_2CH_2PPh_2)_2$] (1),[22] but not as short as the 1.764 (6) Å value found in the iridium–vinylidene complex Ir=C=CH(CO_2Me)(PPr^i_3)$_2$Cl.[25] Other bond lengths and bond angles in the vinylidene derivative 2 are quite similar to those in the methylidene complex 1.

Reactivity Studies. In an attempt to determine the polarity of the α-carbon of the vinylidene unit, that is whether it was susceptible to electrophilic attack (cf A) or nucleophilic attack (cf. B), the reaction with trialkylaluminum reagents (AlR_3) was investigated.[23] The addition of AlR_3 (R = Me, Et) to a toluene solution of the vinylidene 2 results in the loss of the red color and formation of yellow-orange solutions containing a single new product by $^{31}P\{^1H\}$ NMR spectroscopy having the formula Ir(C_2H_2R·AlR_2)[$N(SiMe_2CH_2PPh_2)_2$] (**5a**, R = Me; **5b**, R = Et). The ^1H NMR spectrum of complex **5a** (R = Me) is very straightforward but structurally ambiguous; resonances were observed which indicated that the $AlMe_3$ reagent had transferred a methyl group to the vinylidene ligand to generate an isopropenyl ligand (CMe=CH_2) and that the remaining $AlMe_2$ fragment was still bound in some way to the complex. Similar results were obtained with $AlEt_3$ to give **5b** (R = Et). To ascertain the mode of binding of the aluminum moiety to iridium, we carried out an X-ray crystal structure determination of **5a** (Figure 2).

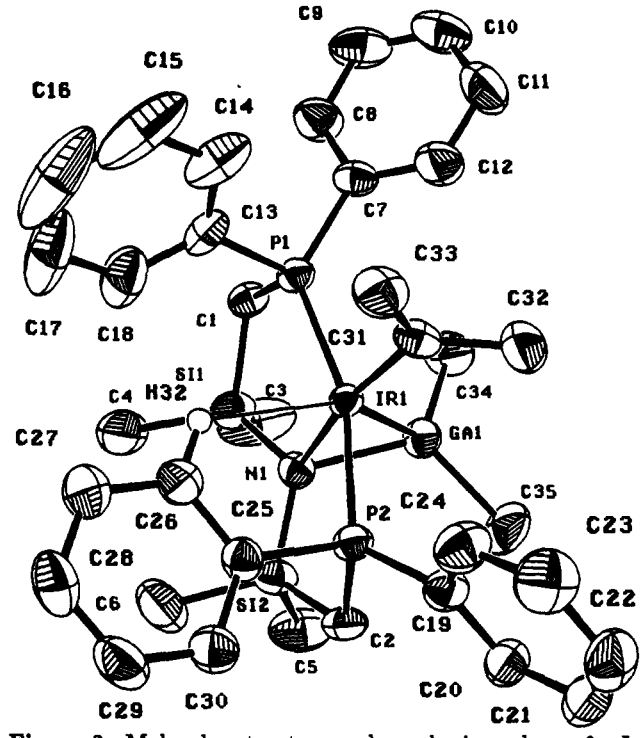

Figure 2. Molecular structure and numbering scheme for Ir($GaMe_2$)CMe=CH_2[$N(SiMe_2CH_2PPh_2)_2$] (**6**). The identical numbering scheme also applies for Ir($AlMe_2$)CMe=CH_2[$N(SiMe_2CH_2PPh_2)_2$] (**5a**), which is isostructural and isomorphous.

The iridium–aluminum complex **5a** has a distorted-square-pyramidal geometry with the isopropenyl ligand in the equatorial plane and an apical $AlMe_2$ group bent bridging over to the amide nitrogen of the ancillary ligand. The Ir–Al bond length of 2.411 (2) Å is slightly shorter than the Rh–Al distance of 2.4581 (8) Å found in CpRh(PMe_3)$_2$($Al_2Me_4Cl_2$).[29] The distances in the Ir–N–Al triangle are informative; the Ir–N bond length is 2.373 (5) Å and the Al–N distance is 1.970 (5) Å, indicative of metal–amine[30,31] lengths typical for an amide ligand bridging two metals. The bond angles within the Ir–N–Al triangle are 66.7 (1)° for Ir–N–Al and 48.6 (1)° for N–Ir–Al. The nitrogen has a distorted-tetrahedral geometry. Also of interest in the solid-state structure is the presence of an agostic C–H···Ir interaction from an ortho hydrogen of one of the phenyl rings to the open site of the square-based pyramid; the Ir–H(32) bond length is 2.68 Å.

This type of reactivity was extended to $GaMe_3$ to produce the product **6**, completely analogous to **5a** but now

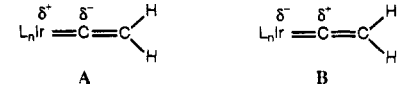

(29) Mayer, J. M.; Calabrese, J. C. *Organometallics* **1985**, *3*, 1292.
(30) Fryzuk, M. D.; MacNeil, P. A.; Rettig, S. J. *J. Am. Chem. Soc.* **1987**, *109*, 2803.
(31) Zaworotko, M. J.; Atwood, J. L. *Inorg. Chem.* **1980**, *19*, 268.

Table II. Final Atomic Coordinates (Fractional) and B_{eq} Values (Å²)[a]

atom	x	y	z	B_{eq}	atom	x	y	z	B_{eq}
			Ir=C=CH$_2$[N(SiMe$_2$CH$_2$PPh$_2$)$_2$]·C$_6$H$_5$CH$_3$						
Ir	0.27800 (1)	0.289787 (8)	0.30647 (1)	2.777 (5)	C(18)	0.6045 (4)	0.1601 (3)	0.5309 (5)	5.3 (2)
P(1)	0.35658 (8)	0.17104 (6)	0.42587 (8)	3.11 (3)	C(19)	0.2761 (4)	0.4734 (2)	0.1226 (3)	3.9 (1)
P(2)	0.18425 (8)	0.40354 (6)	0.18362 (8)	3.23 (3)	C(20)	0.3884 (4)	0.4886 (3)	0.1915 (4)	5.6 (2)
Si(1)	0.2677 (1)	0.09641 (7)	0.1733 (1)	3.85 (4)	C(21)	0.4558 (6)	0.5476 (4)	0.1502 (5)	7.4 (3)
Si(2)	0.1650 (1)	0.25036 (7)	0.0130 (1)	3.81 (4)	C(22)	0.4108 (6)	0.5898 (4)	0.0407 (6)	7.0 (3)
N	0.2319 (3)	0.2057 (2)	0.1542 (3)	3.4 (1)	C(23)	0.3008 (6)	0.5744 (4)	−0.0284 (5)	6.8 (3)
C(1)	0.3879 (3)	0.0846 (2)	0.3212 (4)	3.9 (1)	C(24)	0.2319 (4)	0.5166 (3)	0.0109 (5)	5.9 (2)
C(2)	0.0870 (3)	0.3557 (3)	0.0504 (3)	4.0 (2)	C(25)	0.0891 (3)	0.4816 (2)	0.2534 (3)	3.6 (1)
C(3)	0.1364 (4)	0.0367 (3)	0.1872 (5)	5.8 (2)	C(26)	0.1115 (5)	0.5677 (3)	0.2750 (4)	5.4 (2)
C(4)	0.3336 (5)	0.0433 (3)	0.0469 (5)	6.7 (3)	C(27)	0.0360 (6)	0.6234 (3)	0.3295 (5)	6.2 (2)
C(5)	0.2748 (5)	0.2701 (4)	−0.0804 (5)	6.3 (3)	C(28)	−0.0590 (5)	0.5932 (4)	0.3628 (5)	6.9 (3)
C(6)	0.0472 (5)	0.1845 (3)	−0.0821 (4)	6.2 (2)	C(29)	−0.0797 (6)	0.5086 (4)	0.3435 (7)	8.3 (4)
C(7)	0.2529 (3)	0.1278 (2)	0.5062 (3)	3.6 (1)	C(30)	−0.0061 (5)	0.4534 (3)	0.2895 (6)	6.4 (3)
C(8)	0.1392 (4)	0.1674 (3)	0.4979 (4)	4.8 (2)	C(31)	0.3261 (3)	0.3626 (2)	0.4364 (3)	3.5 (1)
C(9)	0.0605 (5)	0.1323 (4)	0.5570 (5)	6.3 (3)	C(32)	0.3675 (5)	0.4156 (3)	0.5301 (5)	5.4 (2)
C(10)	0.0931 (6)	0.0591 (4)	0.6235 (5)	6.8 (3)	C(33)	0.6976 (5)	0.2858 (3)	0.3080 (5)	6.0 (2)
C(11)	0.2047 (6)	0.0193 (4)	0.6335 (6)	7.6 (3)	C(34)	0.6158 (5)	0.2454 (4)	0.2153 (6)	7.0 (3)
C(12)	0.2860 (5)	0.0529 (3)	0.5756 (5)	6.1 (2)	C(35)	0.6565 (7)	0.1893 (5)	0.1327 (6)	8.2 (4)
C(13)	0.4905 (3)	0.1789 (2)	0.5512 (3)	3.8 (1)	C(36)	0.7772 (8)	0.1709 (4)	0.1395 (7)	8.1 (4)
C(14)	0.4801 (4)	0.2077 (4)	0.6676 (4)	6.1 (2)	C(37)	0.8562 (6)	0.2101 (5)	0.2278 (7)	7.7 (3)
C(15)	0.5806 (6)	0.2168 (4)	0.7624 (5)	7.9 (3)	C(38)	0.8200 (5)	0.2655 (4)	0.3136 (5)	6.2 (2)
C(16)	0.6933 (6)	0.1972 (4)	0.7382 (6)	7.8 (3)	C(39)	0.6579 (7)	0.3481 (4)	0.3964 (8)	9.1 (4)
C(17)	0.7051 (5)	0.1692 (4)	0.6261 (6)	7.4 (3)					
			Ir(η^3-C$_3$H$_5$)I[N(SiMe$_2$CH$_2$PPh$_2$)$_2$]						
Ir	0.61251 (2)	0.36622 (2)	0.371971 (5)	2.347 (7)	C(14)	0.8133 (6)	0.7128 (7)	0.4053 (2)	4.4 (3)
I	0.52708 (4)	0.61584 (4)	0.33721 (1)	3.96 (2)	C(15)	0.8942 (7)	0.8374 (7)	0.4117 (2)	5.8 (3)
P(1)	0.6196 (1)	0.5016 (1)	0.42185 (3)	2.67 (5)	C(16)	0.8873 (8)	0.9117 (7)	0.4418 (2)	5.6 (3)
P(2)	0.5485 (1)	0.2042 (1)	0.32654 (3)	2.97 (5)	C(17)	0.8011 (8)	0.8640 (7)	0.4657 (2)	5.6 (3)
Si(1)	0.3110 (1)	0.4302 (2)	0.40610 (4)	3.30 (6)	C(18)	0.7217 (7)	0.7406 (6)	0.4591 (2)	4.5 (3)
Si(2)	0.3611 (2)	0.1289 (2)	0.38075 (4)	3.64 (6)	C(19)	0.4114 (6)	0.2570 (6)	0.2930 (1)	3.5 (2)
N	0.4068 (4)	0.3059 (5)	0.3859 (1)	2.9 (2)	C(20)	0.3007 (6)	0.3368 (6)	0.3017 (1)	4.2 (3)
C(1)	0.4430 (5)	0.5583 (6)	0.4287 (1)	3.3 (2)	C(21)	0.1897 (7)	0.3677 (8)	0.2780 (2)	5.6 (3)
C(2)	0.4681 (6)	0.0549 (6)	0.3467 (1)	3.8 (2)	C(22)	0.1922 (8)	0.3215 (9)	0.2446 (2)	6.0 (4)
C(3)	0.2035 (6)	0.3504 (8)	0.4393 (2)	5.2 (3)	C(23)	0.3014 (8)	0.2422 (9)	0.2355 (2)	5.8 (4)
C(4)	0.1845 (6)	0.5418 (8)	0.3781 (2)	5.1 (3)	C(24)	0.4106 (7)	0.2088 (7)	0.2596 (1)	4.8 (3)
C(5)	0.403 (1)	0.0128 (7)	0.4194 (2)	6.3 (4)	C(25)	0.6880 (6)	0.1325 (6)	0.3029 (1)	3.8 (2)
C(6)	0.1701 (8)	0.1007 (8)	0.3665 (2)	6.4 (4)	C(26)	0.7453 (7)	−0.0029 (7)	0.3093 (2)	5.2 (3)
C(7)	0.6804 (5)	0.3937 (5)	0.4596 (1)	3.2 (2)	C(27)	0.8613 (8)	−0.0449 (9)	0.2923 (2)	6.6 (4)
C(8)	0.5905 (6)	0.2948 (6)	0.4722 (1)	3.7 (2)	C(28)	0.9147 (9)	0.041 (1)	0.2690 (2)	7.1 (5)
C(9)	0.6356 (7)	0.2060 (7)	0.4992 (2)	4.5 (3)	C(29)	0.8555 (8)	0.1749 (8)	0.2618 (2)	5.8 (4)
C(10)	0.7715 (7)	0.2143 (7)	0.5142 (1)	4.6 (3)	C(30)	0.7451 (7)	0.2217 (7)	0.2790 (2)	4.8 (3)
C(11)	0.8614 (7)	0.3112 (7)	0.5016 (2)	5.0 (3)	C(31)	0.7526 (6)	0.2005 (7)	0.3932 (1)	4.1 (3)
C(12)	0.8170 (6)	0.4021 (6)	0.4745 (1)	3.9 (2)	C(32)	0.8272 (5)	0.3298 (7)	0.3871 (2)	4.1 (3)
C(13)	0.7264 (5)	0.6645 (5)	0.4289 (1)	3.3 (2)	C(33)	0.8235 (5)	0.3854 (7)	0.3542 (2)	4.3 (3)
			Ir(AlMe$_2$)CMe=CH$_2$[N(SiMe$_2$CH$_2$PPh$_2$)$_2$]						
Ir(1)	0.25719 (1)	0.37091 (2)	0.43809 (1)	2.013 (7)	C(15)	0.4842 (6)	0.064 (2)	0.5818 (5)	8.5 (6)
P(1)	0.30275 (8)	0.3232 (1)	0.55026 (7)	2.39 (5)	C(16)	0.446 (1)	−0.061 (1)	0.5593 (6)	9.4 (7)
P(2)	0.20919 (9)	0.3447 (1)	0.32316 (7)	2.46 (5)	C(17)	0.3712 (8)	−0.068 (1)	0.5402 (5)	7.7 (5)
Si(1)	0.1309 (1)	0.2448 (2)	0.5069 (1)	3.86 (7)	C(18)	0.3267 (5)	0.0433 (7)	0.5393 (4)	5.0 (3)
Si(2)	0.0706 (1)	0.2739 (2)	0.35552 (9)	3.32 (6)	C(19)	0.2369 (3)	0.4454 (6)	0.2637 (3)	2.7 (2)
Al(1)	0.1600 (1)	0.5252 (2)	0.4451 (1)	2.95 (6)	C(20)	0.1864 (4)	0.5295 (6)	0.2153 (3)	3.5 (2)
N(1)	0.1319 (3)	0.3286 (5)	0.4352 (2)	2.6 (2)	C(21)	0.2115 (4)	0.6074 (6)	0.1723 (3)	4.1 (3)
C(1)	0.2253 (3)	0.2722 (6)	0.5778 (3)	3.0 (2)	C(22)	0.2853 (5)	0.6015 (7)	0.1770 (4)	4.5 (3)
C(2)	0.1052 (3)	0.3496 (6)	0.2913 (3)	3.3 (2)	C(23)	0.3351 (4)	0.5184 (8)	0.2242 (4)	4.8 (3)
C(3)	0.0539 (5)	0.314 (1)	0.5343 (5)	8.3 (5)	C(24)	0.3114 (4)	0.4387 (8)	0.2671 (3)	4.0 (3)
C(4)	0.1129 (7)	0.057 (1)	0.4982 (5)	9.2 (5)	C(25)	0.2313 (3)	0.1692 (6)	0.3060 (3)	2.8 (2)
C(5)	−0.0282 (4)	0.334 (1)	0.3380 (4)	5.8 (4)	C(26)	0.2761 (4)	0.0866 (6)	0.3591 (3)	3.8 (2)
C(6)	0.0661 (6)	0.0840 (9)	0.3396 (4)	6.2 (4)	C(27)	0.2910 (5)	−0.0496 (7)	0.3478 (4)	5.1 (3)
C(7)	0.3629 (3)	0.4314 (6)	0.6191 (3)	2.9 (2)	C(28)	0.2623 (5)	−0.1009 (7)	0.2844 (4)	5.1 (3)
C(8)	0.3779 (4)	0.3933 (8)	0.6849 (3)	4.5 (3)	C(29)	0.2203 (5)	−0.0226 (7)	0.2314 (4)	4.6 (3)
C(9)	0.4226 (5)	0.471 (1)	0.7381 (3)	5.2 (3)	C(30)	0.2038 (4)	0.1125 (7)	0.2422 (3)	4.0 (3)
C(10)	0.4537 (5)	0.5924 (9)	0.7264 (4)	5.3 (3)	C(31)	0.3565 (3)	0.4451 (6)	0.4368 (3)	2.7 (2)
C(11)	0.4403 (5)	0.6326 (9)	0.6615 (4)	6.1 (4)	C(32)	0.3576 (4)	0.5968 (7)	0.4223 (4)	4.1 (3)
C(12)	0.3956 (5)	0.5504 (8)	0.6078 (3)	4.5 (3)	C(33)	0.4200 (4)	0.3705 (7)	0.4457 (3)	4.0 (3)
C(13)	0.3616 (4)	0.1696 (6)	0.5600 (3)	3.4 (2)	C(34)	0.1751 (5)	0.6161 (7)	0.5311 (4)	5.1 (3)
C(14)	0.4406 (5)	0.179 (1)	0.5820 (4)	5.2 (3)	C(35)	0.1067 (5)	0.6557 (7)	0.3714 (4)	5.3 (3)
			Ir(GaMe$_2$)CMe=CH$_2$[N(SiMe$_2$CH$_2$PPh$_2$)$_2$]						
Ir(1)	0.25713 (1)	0.36931 (2)	0.438897 (8)	2.136 (6)	C(1)	0.2250 (3)	0.2726 (5)	0.5785 (2)	3.0 (2)
Ga(1)	0.16081 (3)	0.53079 (6)	0.44645 (3)	3.18 (2)	C(2)	0.1052 (3)	0.3498 (5)	0.2924 (2)	3.3 (2)
P(1)	0.30252 (7)	0.3223 (1)	0.55079 (6)	2.55 (4)	C(3)	0.0543 (4)	0.309 (1)	0.5349 (4)	8.4 (4)
P(2)	0.20914 (7)	0.3442 (1)	0.32416 (6)	2.61 (4)	C(4)	0.1148 (5)	0.0531 (8)	0.4990 (4)	9.1 (4)
Si(1)	0.13126 (8)	0.2415 (2)	0.50741 (7)	3.94 (6)	C(5)	−0.0283 (3)	0.3344 (8)	0.3397 (3)	6.0 (3)
Si(2)	0.07052 (8)	0.2722 (2)	0.35646 (7)	3.51 (5)	C(6)	0.0644 (4)	0.0833 (7)	0.3390 (3)	6.3 (3)
N(1)	0.1330 (2)	0.3233 (4)	0.4356 (2)	2.7 (1)	C(7)	0.3628 (3)	0.4308 (5)	0.6195 (2)	3.1 (2)

Table II (Continued)

atom	x	y	z	B_{eq}	atom	x	y	z	B_{eq}
C(8)	0.3771 (3)	0.3921 (6)	0.6854 (3)	4.7 (2)	C(22)	0.2857 (4)	0.6017 (6)	0.1787 (3)	4.8 (3)
C(9)	0.4223 (4)	0.4724 (8)	0.7380 (3)	5.7 (3)	C(23)	0.3357 (3)	0.5178 (7)	0.2260 (3)	5.1 (3)
C(10)	0.4529 (4)	0.5926 (8)	0.7261 (3)	5.6 (3)	C(24)	0.3124 (3)	0.4382 (6)	0.2682 (3)	4.1 (2)
C(11)	0.4400 (4)	0.6332 (7)	0.6611 (3)	6.2 (3)	C(25)	0.2315 (3)	0.1678 (5)	0.3072 (2)	2.8 (2)
C(12)	0.3947 (4)	0.5510 (7)	0.6080 (3)	4.9 (3)	C(26)	0.2763 (3)	0.0857 (6)	0.3598 (3)	4.1 (2)
C(13)	0.3627 (3)	0.1707 (5)	0.5613 (2)	3.5 (2)	C(27)	0.2906 (4)	−0.0498 (6)	0.3495 (3)	5.0 (3)
C(14)	0.4407 (4)	0.1808 (8)	0.5826 (3)	5.5 (3)	C(28)	0.2620 (4)	−0.1020 (6)	0.2861 (3)	5.1 (3)
C(15)	0.4839 (5)	0.063 (1)	0.5821 (4)	8.7 (5)	C(29)	0.2198 (4)	−0.0217 (6)	0.2329 (3)	4.6 (2)
C(16)	0.4489 (8)	−0.059 (1)	0.5611 (5)	10.6 (7)	C(30)	0.2043 (3)	0.1110 (5)	0.2431 (2)	3.8 (2)
C(17)	0.3706 (7)	−0.0709 (8)	0.5411 (4)	8.4 (5)	C(31)	0.3573 (3)	0.4443 (5)	0.4383 (2)	3.0 (2)
C(18)	0.3279 (4)	0.0436 (6)	0.5402 (3)	5.5 (3)	C(32)	0.3577 (4)	0.5962 (6)	0.4237 (3)	4.7 (2)
C(19)	0.2371 (3)	0.4443 (5)	0.2646 (2)	3.1 (2)	C(33)	0.4204 (3)	0.3712 (6)	0.4465 (3)	4.3 (2)
C(20)	0.1873 (3)	0.5288 (5)	0.2167 (2)	3.6 (2)	C(34)	0.1739 (4)	0.6172 (6)	0.5338 (3)	5.1 (3)
C(21)	0.2113 (4)	0.6072 (6)	0.1739 (3)	4.4 (2)	C935)	0.1065 (4)	0.6578 (6)	0.3715 (3)	5.5 (3)

[a] $B_{eq} = {}^{8}/_{3}\pi^{2}\sum\sum U_{ij}a_{i}a_{j}(\mathbf{a}_{i}\cdot\mathbf{a}_{j})$.

Scheme III

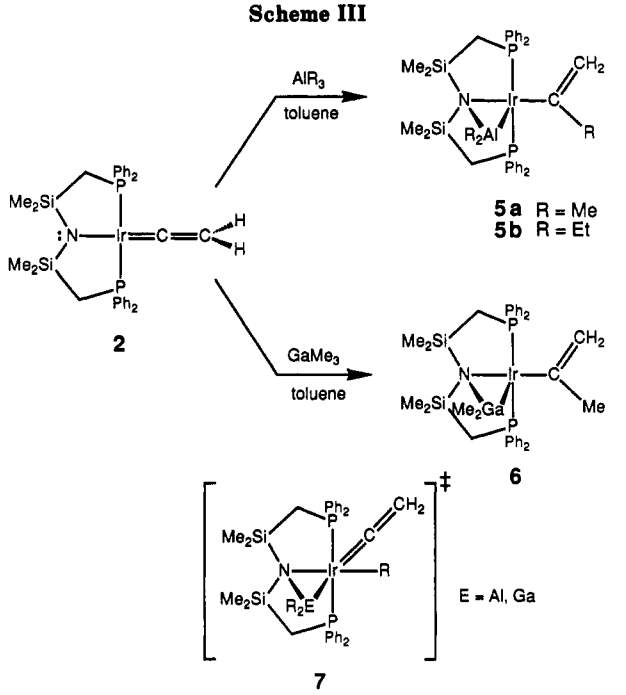

having a $GaMe_2$ fragment directly bound to the iridium via a bridging amide. The single-crystal X-ray analysis of **6** (Figure 2) showed it to be isomorphous and isostructural with the aluminum derivative **5a**; most of the bond lengths are nearly identical except for the slightly longer Ir–Ga and Ga–N distances of 2.4480 (7) and 2.076 (4) Å, respectively. Within the Ir–N–Ga triangle, the Ir–N–Ga bond angle (66.8 (1)°) is identical with that found in the aluminum derivative, with the remaining angles of the triangle slightly different due to the differences in bond lengths between the two derivatives.

A reasonable pathway for the formation of this species probably involves oxidative addition[32-34] of the ER_3 (E = Al, Ga) monomer to the 16-electron, formally iridium(I) vinylidene **2** to generate the transient species **7** having an ER_2 ligand, an alkyl, and the vinylidene as in Scheme III. Migratory insertion of the vinylidene and the alkyl ligand generates the isopropenyl unit. An extension to trialkylborane reagents (BR_3) was attempted; however, no reaction of the vinylidene **2** with BEt_3 was observed even with heating. Other organo derivatives of group 13 were not investigated.

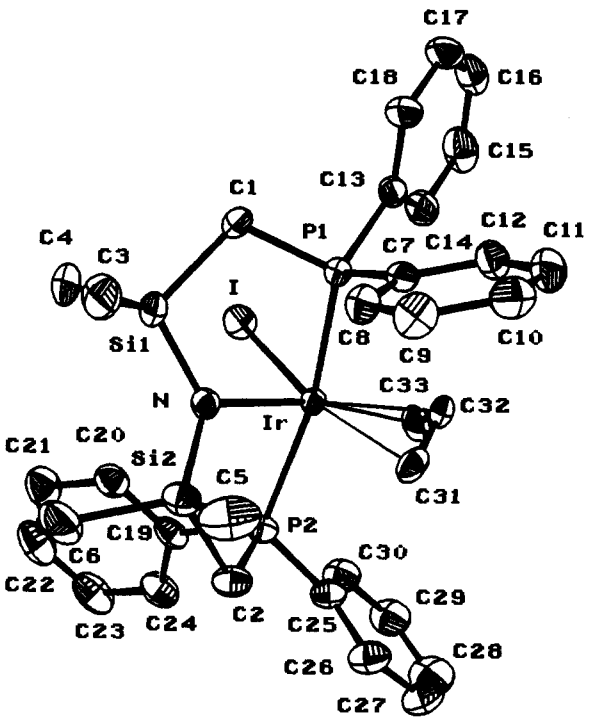

Figure 3. Molecular structure and numbering scheme for Ir-(η^3-C_3H_5)I[$N(SiMe_2CH_2PPh_2)_2$] (**8**).

Prior to the migratory insertion step of the vinylidene unit in the presumed but not observed intermediate **7**, oxidative addition of AlR_3 and $GaMe_3$ was invoked as a necessary means of introducing the alkyl ligand. While this type of oxidative-addition reaction does have precedent,[32-34] a simpler sequence would involve oxidative addition of alkyl halides, a well-known reaction especially for square-planar complexes of iridium(I).[35,36]

The addition of CH_3I to the vinylidene complex **2** results in the slow formation (48 h) of the allyl–iodide complex **8** in virtually quantitative yield (by $^{31}P\{^1H\}$ NMR spectroscopy) (eq 1). The allyl ligand is bound asymmetrically

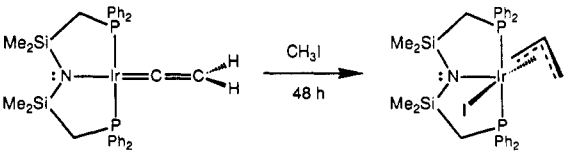

(1)

(32) Vazquez de Miguel, A.; Gomez, M.; Isobe, K.; Taylor, B. F.; Mann, B. E.; maitlis, P. M. *Organometallics* **1983**, *2*, 1724.
(33) Thorn, D. L.; Harlow, R. L. *J. Am. Chem. Soc.* **1989**, *111*, 2575.
(34) Fischer, R. A.; Kaesz, H. D.; Khan, S. I.; Müller, H. *Inorg. Chem.* **1990**, *29*, 1601.
(35) Collman, J. P.; Hegedus, L. S.; Norton, J. R.; Finke, R. G. In *Principles and Applications of Organotransition Metal Chemistry*; University Science Books: Mill Valley, CA, 1987; Chapter 5, p 306.
(36) Labinger, J. A.; Osborn, J. A. *Inorg. Chem.* **1980**, *19*, 3230–3236.

Table III. Selected Bond Lengths (Å) with Estimated Standard Deviations

$Ir{=}C{=}CH_2[N(SiMe_2CH_2PPh_2)_2]{\cdot}C_6H_5CH_3$			
Ir–C(31)	1.806 (4)	Si(1)–N	1.718 (3)
Ir–N	2.088 (3)	Si(1)–C(4)	1.871 (5)
Ir–P(1)	2.299 (1)	Si(1)–C(3)	1.872 (5)
Ir–P(2)	2.299 (1)	Si(1)–C(1)	1.884 (4)
P(1)–C(1)	1.806 (4)	Si(2)–N	1.714 (3)
P(1)–C(7)	1.820 (4)	Si(2)–C(5)	1.854 (5)
P(1)–C(13)	1.827 (4)	Si(2)–C(6)	1.865 (5)
P(2)–C(2)	1.808 (4)	Si(2)–C(2)	1.876 (4)
P(2)–C(19)	1.819 (4)	C(31)–C(32)	1.324 (6)
P(2)–C(25)	1.830 (4)		
$Ir(\eta^3\text{-}C_3H_5)I[N(SiMe_2CH_2PPh_2)_2]$			
Ir–A[a]	1.886 (3)	P(2)–C(25)	1.818 (6)
Ir–C(32)	2.113 (5)	P(2)–C(19)	1.838 (5)
Ir–C(31)	2.156 (5)	Si(1)–N	1.712 (5)
Ir–N	2.163 (4)	Si(1)–C(4)	1.870 (6)
Ir–C(33)	2.202 (5)	Si(1)–C(3)	1.884 (6)
Ir–P(1)	2.322 (1)	Si(1)–C(1)	1.893 (5)
Ir–P(2)	2.369 (2)	Si(2)–N	1.705 (4)
Ir–I	2.771 (1)	Si(2)–C(5)	1.874 (7)
P(1)–C(1)	1.813 (5)	Si(2)–C(6)	1.881 (7)
P(1)–C(13)	1.830 (5)	Si(2)–C(2)	1.886 (6)
P(1)–C(7)	1.838 (5)	C(31)–C(32)	1.427 (8)
P(2)–C(2)	1.801 (6)	C(32)–C(33)	1.386 (8)
$Ir(AlMe_2)CMe{=}CH_2[N(SiMe_2CH_2PPh_2)_2]$			
Ir(1)–C(31)	2.014 (6)	Si(1)–C(4)	1.85 (1)
Ir(1)–P(1)	2.273 (2)	Si(1)–C(3)	1.88 (1)
Ir(1)–P(2)	2.294 (2)	Si(1)–C(1)	1.878 (6)
Ir(1)–N(1)	2.373 (5)	Si(2)–N(1)	1.747 (5)
Ir(1)–Al(1)	2.411 (2)	Si(2)–C(5)	1.851 (8)
Ir(1)–H(32)	2.68	Si(2)–C(6)	1.869 (8)
P(1)–C(7)	1.819 (6)	Si(2)–C(2)	1.872 (6)
P(1)–C(13)	1.822 (6)	Al(1)–C(34)	1.961 (7)
P(1)–C(1)	1.830 (6)	Al(1)–N(1)	1.970 (5)
P(2)–C(2)	1.819 (6)	Al(1)–C(35)	1.979 (8)
P(2)–C(25)	1.822 (6)	C(31)–C(33)	1.348 (9)
P(2)–C(19)	1.825 (6)	C(31)–C(32)	1.505 (8)
Si(1)–N(1)	1.739 (5)		
$Ir(AlMe_2)CMe{=}CH_2[N(SiMe_2CH_2PPh_2)_2]$			
Ir(1)–Ga(1)	2.4480 (7)	P(2)–C(19)	1.830 (5)
Ir(1)–P(1)	2.277 (1)	P(2)–C(25)	1.835 (5)
Ir(1)–P(2)	2.301 (1)	Si(1)–N(1)	1.744 (4)
Ir(1)–N(1)	2.353 (4)	Si(1)–C(1)	1.884 (5)
Ir(1)–C(31)	2.025 (5)	Si(1)–C(3)	1.872 (7)
Ir(1)–H(32)	2.68	Si(1)–C(4)	1.856 (8)
Ga(1)–N(1)	2.076 (4)	Si(2)–N(1)	1.744 (4)
Ga(1)–C(34)	1.984 (6)	Si(2)–C(2)	1.881 (5)
Ga(1)–C(35)	1.987 (6)	Si(2)–C(5)	1.860 (6)
P(1)–C(1)	1.831 (5)	Si(2)–C(6)	1.869 (7)
P(1)–C(7)	1.828 (5)	C(31)–C(32)	1.511 (7)
P(1)–C(13)	1.823 (5)	C(31)–C(33)	1.339 (7)
P(2)–C(2)	1.821 (5)		

[a] Here and elsewhere "A" refers to the unweighted centroid of the allyl ligand.

and rigidly, as evidenced by the ^1H NMR spectrum, which shows five different resonances for the five protons of the $\eta^3\text{-}C_3H_5$ unit. In addition, the $^{31}P\{^1H\}$ NMR spectrum of **8** consists of an AB pattern due to inequivalent phosphorus donors; a phosphorus–phosphorus coupling constant ($^2J_{PP}$) of 425 Hz is indicative of trans-disposed phosphines and, therefore, a meridional geometry for the ancillary tridentate ligand.

The solid-state structure of the allyl derivative **8** as determined by single-crystal X-ray analysis is shown in Figure 3. The molecule has a distorted-octahedral geometry, assuming that the allyl ligand occupies two cis sites. The Ir–C bond lengths show the asymmetric nature of the binding since the lengths vary from 2.113 (5) to 2.202 (5) Å, with Ir–C(32), the bond to the central carbon, being the shortest. The C–C bond lengths are also quite different: C(31)–C(32) is 1.427 (8) Å and C(32)–C(33) is 1.386 (8) Å.

Scheme IV

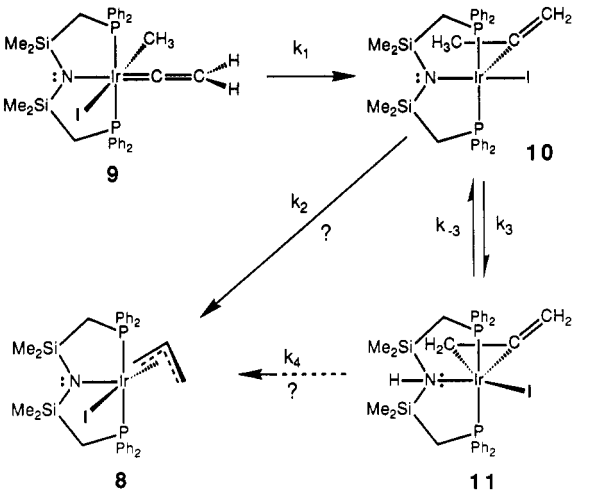

All other bond lengths are similar to those in other structures with this ligand system. Thus, the solution structure, as determined by ^1H and $^{31}P\{^1H\}$ NMR spectroscopy, is completely consistent with the solid-state structure.

The formation of the C_3 allyl fragment requires a C–C bond-forming step along with a hydrogen-transfer process. When the reaction of CH_3I with **2** was monitored by NMR spectroscopy, a number of presumed intermediates could be detected as a function of time to provide mechanistic information on this process (detailed kinetic studies will be reported separately). Labeling studies were also performed to confirm the fate of the various species in solution.

Addition of CH_3I to the vinylidene complex **2** at −30 °C results in the formation of the first detectable intermediate, the methyl–vinylidene–iodide complex **9**; the formation of this species is quantitative by NMR spectroscopy after about 10 min at −30 °C. The methyl–iodide adduct **9**

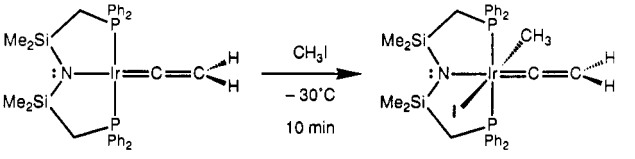

(2)

could not be isolated, and so its structure was inferred spectroscopically. Particularly diagnostic in the ^1H NMR spectrum of **9** is the triplet at 1.92 ppm for the iridium-bound methyl (Ir–CH_3) and the two singlets at 5.10 and 5.45 ppm for the now-inequivalent vinylidene protons; the analogous reaction of $^{13}CH_3I$ generates a doublet of triplets for the Ir–$^{13}CH_3$ moiety with $^1J_{C,H}$ = 130 Hz. A trans oxidative addition of CH_3I is assumed on the basis of previous work and literature precedent.[26,37] This complex is stable for short periods of time below 0 °C in solution; however, if it is warmed above this temperature, a sequence of reactions occurs which ultimately results in the formation of the allyl iodide **8**. Shown in Scheme IV is a plausible mechanism for the transformation of the methyl–iodide intermediate **9** to the allyl–iodide **8**. All of the species in this scheme were detected and characterized by NMR spectroscopy; although solution spectra of pure **9** and pure **8** could be obtained at the beginning and end of the reaction, respectively, the intermediates **10** and **11** were only observed as components in a mixture.

(37) Fryzuk, M. D.; Bhangu, K. *Organometallics* **1989**, *8*, 722–726.

Table IV. Selected Bond Angles (deg) with Estimated Standard Deviations in Parentheses

			Ir=C=CH$_2$[N(SiMe$_2$CH$_2$PPh$_2$)$_2$]·C$_6$H$_5$CH$_3$				
C(31)-Ir-N	176.8 (1)	C(7)-P(1)-C(13)	101.9 (2)	N-Si(1)-C(4)	113.7 (2)	N-Si(2)-C(2)	105.3 (2)
C(31)-Ir-P(1)	91.5 (1)	C(7)-P(1)-Ir	114.4 (1)	N-Si(1)-C(3)	112.6 (2)	C(5)-Si(2)-C(6)	108.9 (3)
C(31)-Ir-P(2)	91.1 (1)	C(13)-P(1)-Ir	119.9 (1)	N-Si(1)-C(1)	106.0 (2)	C(5)-Si(2)-C(2)	109.9 (2)
N-Ir-P(1)	88.25 (9)	C(2)-P(2)-C(19)	106.5 (2)	C(4)-Si(1)-C(3)	108.3 (3)	C(6)-Si(2)-C(2)	106.8 (2)
N-Ir-P(2)	89.35 (9)	C(2)-P(2)-C(25)	106.6 (2)	C(4)-Si(1)-C(1)	106.4 (2)	Si(2)-N-Si(1)	122.8 (2)
P(1)-Ir-P(2)	175.22 (5)	C(2)-P(2)-Ir	105.9 (1)	C(3)-Si(1)-C(1)	109.4 (2)	Si(2)-N-Ir	117.7 (2)
C(1)-P(1)-C(7)	104.4 (2)	C(19)-P(2)-C(25)	102.4 (2)	N-Si(2)-C(5)	112.6 (2)	Si(1)-N-Ir	119.4 (2)
C(1)-P(1)-C(13)	107.9 (2)	C(19)-P(2)-Ir	118.6 (1)	N-Si(2)-C(6)	113.2 (2)	C(32)-C(31)-Ir	176.7 (4)
C(1)-P(1)-Ir	107.2 (1)	C(25)-P(2)-Ir	116.1 (1)				
			Ir(η^3-C$_3$H$_5$)I[N(SiMe$_2$CH$_2$PPh$_2$)$_2$]				
A-Ir-N	140.5 (2)	C(1)-P(1)-C(13)	104.7 (2)	C(25)-P(2)-Ir	117.6 (2)	N-Si(2)-C(2)	106.5 (2)
A-Ir-P(1)	95.7 (1)	C(1)-P(1)-C(7)	105.7 (2)	C(19)-P(2)-Ir	119.3 (2)	C(5)-Si(2)-C(6)	106.9 (4)
A-Ir-P(2)	94.9 (1)	C(1)-P(1)-Ir	109.0 (2)	N-Si(1)-C(4)	116.4 (3)	C(5)-Si(2)-C(2)	106.0 (3)
A-Ir-I	123.4 (1)	C(13)-P(1)-C(7)	101.2 (2)	N-Si(1)-C(3)	114.0 (3)	C(6)-Si(2)-C(2)	108.4 (3)
N-Ir-P(1)	83.3 (1)	C(13)-P(1)-Ir	123.2 (2)	N-Si(1)-C(1)	106.0 (2)	Si(2)-N-Si(1)	124.0 (2)
N-Ir-P(2)	81.2 (1)	C(7)-P(1)-Ir	111.7 (2)	C(4)-Si(1)-C(3)	104.9 (3)	Si(2)-N-Ir	116.7 (2)
N-Ir-I	96.1 (1)	C(2)-P(2)-C(25)	107.8 (3)	C(4)-Si(1)-C(1)	107.3 (3)	Si(1)-N-Ir	118.8 (2)
P(1)-Ir-P(2)	164.44 (5)	C(2)-P(2)-C(19)	102.3 (3)	C(3)-Si(1)-C(1)	107.8 (3)	P(1)-C(1)-Si(1)	109.9 (3)
P(1)-Ir-I	87.09 (5)	C(2)-P(2)-Ir	104.3 (2)	N-Si(2)-C(5)	115.0 (3)	P(2)-C(2)-Si(2)	108.3 (3)
P(2)-Ir-I	96.54 (5)	C(25)-P(2)-C(19)	104.0 (3)	N-Si(2)-C(6)	113.7 (3)	C(33)-C(32)-C(31)	119.9 (5)
			Ir(AlMe$_2$)CMe=CH$_2$[N(SiMe$_2$CH$_2$PPh$_2$)$_2$]				
C(31)-Ir(1)-P(1)	95.7 (2)	Al(1)-Ir(1)-H(32)	149.9	N(1)-Si(1)-C(3)	111.6 (4)	N(1)-Al(1)-C(35)	119.8 (3)
C(31)-Ir(1)-P(2)	91.4 (2)	C(7)-P(1)-C(13)	102.1 (3)	N(1)-Si(1)-C(1)	109.1 (3)	N(1)-Al(1)-Ir(1)	64.7 (1)
C(31)-Ir(1)-N(1)	168.8 (2)	C(7)-P(1)-C(1)	103.1 (3)	C(4)-Si(1)-C(3)	104.5 (6)	C(35)-Al(1)-Ir(1)	121.3 (3)
C(31)-Ir(1)-Al(1)	120.6 (2)	C(7)-P(1)-Ir(1)	127.7 (2)	C(4)-Si(1)-C(1)	107.7 (4)	Si(1)-N(1)-Si(2)	119.8 (3)
C(31)-Ir(1)-H(32)	87.7	C(13)-P(1)-C(1)	105.4 (3)	C(3)-Si(1)-C(1)	107.9 (4)	Si(1)-N(1)-Al(1)	116.6 (3)
P(1)-Ir(1)-P(2)	161.86 (5)	C(13)-P(1)-Ir(1)	105.2 (2)	N(1)-Si(2)-C(5)	110.6 (3)	Si(1)-N(1)-Ir(1)	113.2 (2)
P(1)-Ir(1)-N(1)	88.5 (1)	C(1)-P(1)-Ir(1)	111.1 (2)	N(1)-Si(2)-C(6)	116.4 (3)	Si(2)-N(1)-Al(1)	116.9 (3)
P(1)-Ir(1)-Al(1)	93.39 (6)	C(2)-P(2)-C(25)	104.1 (3)	N(1)-Si(2)-C(2)	108.1 (3)	Si(2)-N(1)-Ir(1)	111.6 (2)
P(1)-Ir(1)-H(32)	93.7	C(2)-P(2)-C(19)	105.8 (3)	C(5)-Si(2)-C(6)	107.5 (4)	Al(1)-N(1)-Ir(1)	66.7 (1)
P(2)-Ir(1)-N(1)	87.7 (1)	C(2)-P(2)-Ir(1)	109.8 (2)	C(5)-Si(2)-C(2)	108.9 (3)	C(33)-C(31)-C(32)	118.4 (6)
P(2)-Ir(1)-Al(1)	97.40 (6)	C(25)-P(2)-C(19)	102.4 (3)	C(6)-Si(2)-C(2)	105.0 (3)	C(33)-C(31)-Ir(1)	125.8 (5)
P(2)-Ir(1)-H(32)	66.9	C(25)-P(2)-Ir(1)	106.9 (2)	C(34)-Al(1)-N(1)	118.4 (3)	C(32)-C(31)-Ir(1)	115.8 (4)
N(1)-Ir(1)-Al(1)	48.6 (1)	C(19)-P(2)-Ir(1)	125.8 (2)	C(34)-Al(1)-C(35)	108.2 (3)	Ir(1)-H(32)-C(26)	123.3
N(1)-Ir(1)-H(32)	102.4	N(1)-Si(1)-C(4)	115.7 (4)	C(34)-Al(1)-Ir(1)	119.2 (2)		
			Ir(GaMe$_2$)CMe=CH$_2$[N(SiMe$_2$CH$_2$PPh$_2$)$_2$]				
Ga(1)-Ir(1)-P(1)	93.38 (4)	C(31)-Ir(1)-H(32)	87.5	Ir(1)-P(2)-C(19)	126.1 (2)	C(2)-Si(2)-C(5)	108.5 (3)
Ga(1)-Ir(1)-P(2)	97.46 (3)	Ir(1)-Ga(1)-N(1)	62.0 (1)	Ir(1)-P(2)-C(25)	106.4 (2)	C(2)-Si(2)-C(6)	105.1 (3)
Ga(1)-Ir(1)-N(1)	51.2 (1)	Ir(1)-Ga(1)-C(34)	119.8 (2)	C(2)-P(2)-C(19)	105.6 (2)	C(5)-Si(2)-C(6)	107.3 (3)
Ga(1)-Ir(1)-C(31)	118.9 (1)	Ir(1)-Ga(1)-C(34)	121.2 (2)	C(2)-P(2)-C(25)	104.3 (2)	Ir(1)-N(1)-Ga(1)	66.8 (1)
Ga(1)-Ir(1)-H(32)	151.7	N(1)-Ga(1)-C(34)	117.1 (2)	C(19)-P(2)-C(25)	102.3 (2)	Ir(1)-N(1)-Si(1)	113.7 (2)
P(1)-Ir(1)-P(2)	162.33 (4)	N(1)-Ga(1)-C(35)	118.7 (2)	N(1)-Si(1)-C(1)	109.0 (2)	Ir(1)-N(1)-Si(2)	112.9 (2)
P(1)-Ir(1)-N(1)	88.7 (1)	C(34)-Ga(1)-C(35)	110.4 (3)	N(1)-Si(1)-C(3)	112.7 (3)	Ga(1)-N(1)-Si(1)	115.5 (2)
P(1)-Ir(1)-C(31)	95.1 (1)	Ir(1)-P(1)-C(1)	111.1 (1)	N(1)-Si(1)-C(4)	114.9 (3)	Ga(1)-N(1)-Si(2)	116.0 (2)
P(1)-Ir(1)-H(32)	94.2	Ir(1)-P(1)-C(7)	127.9 (2)	C(1)-Si(1)-C(3)	106.9 (3)	Si(1)-N(1)-Si(2)	120.3 (2)
P(2)-Ir(1)-N(1)	87.3 (1)	Ir(1)-P(1)-C(13)	105.5 (2)	C(1)-Si(1)-C(4)	108.1 (3)	Ir(1)-C(31)-C(32)	115.5 (4)
P(2)-Ir(1)-C(31)	91.8 (1)	C(1)-P(1)-C(7)	102.8 (2)	C(3)-Si(1)-C(4)	104.9 (5)	Ir(1)-C(31)-C(33)	126.2 (4)
P(2)-Ir(1)-H(32)	69.9	C(1)-P(1)-C(13)	106.2 (2)	N(1)-Si(2)-C(2)	107.8 (2)	C(32)-C(31)-C(33)	118.3 (5)
N(1)-Ir(1)-C(31)	169.7 (2)	C(7)-P(1)-C(13)	101.2 (2)	N(1)-Si(2)-C(5)	111.3 (3)	Ir(1)-H(32)-C(26)	123.5
N(1)-Ir(1)-H(32)	101.8	Ir(1)-P(2)-C(2)	110.0 (2)	N(1)-Si(2)-C(6)	116.4 (3)		

The isopropenyl–iodide intermediate **10** was characterized by the typical resonances for the Ir—CMe=CH$_2$ unit in the ^{1}H NMR spectrum: two broad singlets at 4.72 and 3.88 ppm for the two vinyl protons (Ir—CMe=CH_2) are observed which, for the reaction with $^{13}CH_3I$, are further split into doublets ($^3J_{C_{trans}}$ = 9 Hz; $^3J_{C_{cis}} \approx$ 2 Hz), and the vinylic methyl (Ir–C(CH_3)=CH$_2$) is seen as a singlet at 1.1 ppm further split into a doublet ($^1J_{C,H}$ = 126 Hz) for the $^{13}CH_3$-labeled material. These resonances are consistent with other similar complexes containing this fragment.[20]

The allene–amine derivative **11** was more difficult to characterize, as its concentration did not build up to a large extent during the reaction seqeunce outlined in Scheme IV. Its identity is inferred from a singlet in the $^{31}P\{^1H\}$ NMR spectrum and resonances typical for a coordinated allene moiety[38] in the ^{1}H NMR spectrum: for the coordinated end of the allene, Ir(η^2-H$_2$C=C), there is a singlet at 1.60 ppm which splits into a doublet ($^1J_{C,H}$ = 155 Hz) upon reaction with $^{13}CH_3I$, and the protons of the uncoordinated end, C=CH$_2$, resonate as a broad singlet at 6.06 ppm. This latter resonance is not affected when the reaction is performed with either $^{13}CH_3I$ or CD$_3$I. In addition, there are two silylmethyl (Si(CH$_3$)$_2$) resonances for the tridentate ancillary ligand that indicate inequivalent environments above and below the plane of the ligand. That complex **11** has a coordinated amine in the backbone could not be directly substantiated from spectroscopic data; in the mixture of complexes that are present when **11** is formed (see Scheme IV), there was neither an N–H resonance in the ^{1}H NMR spectrum nor a clear N–H stretch in the IR spectrum that could be assigned to such a feature. However, such evidence may be hidden because of the complexity of these spectra due to overlap of resonances/stretches of the various species present.

Most noticeably absent in the ^{1}H NMR spectrum was an upfield peak characteristic of an iridium–hydride moiety. This was at first surprising, since there is precedent[39-41] for the rearrangement of an isopropenyl group

(38) The preparation of Ir(η^2-H$_2$C=C=CH$_2$)[N(SiMe$_2$CH$_2$PPh$_2$)$_2$] is described in: Joshi, K. Ph.D. Dissertation, 1990.

Scheme V

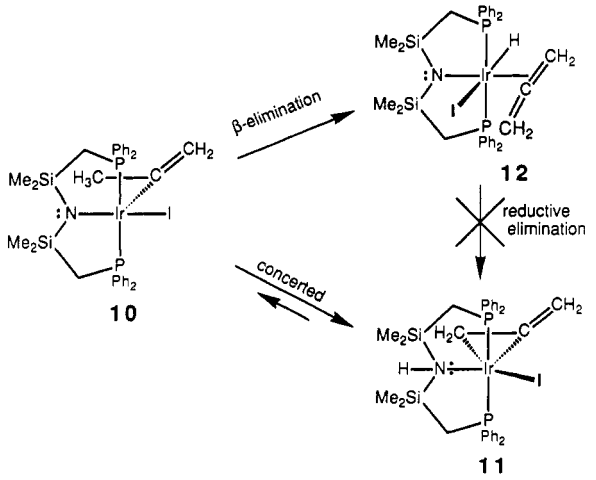

to an allyl ligand via an intermediate allene–hydride species; however, all the evidence in the literature for the formation of an allene–hydride species via β-elimination from an isopropenyl moiety is indirect, based entirely on product analysis. To account for the formation of the allene–amine derivative **11**, it is suggested that β-proton abstraction by the basic amide donor of the ancillary ligand from the methyl of the isopropenyl unit is operative. That this is a concerted process and *not* a two-step procedure involving the intermediacy of the allene–hydride complex **12** followed by reductive elimination (Scheme V) is supported by the following evidence: the aluminum and gallium complexes **5** and **6** contain the isopropenyl unit and do not rearrange presumably because the basic amide is involved in bonding to the respective group 13 elements.

The mechanism in Scheme IV is ambiguous in that two distinct pathways are shown that produce the allyl product **8**; one pathway involves transformation of the isopropenyl complex **10** via the k_2 step, while the other involves the intermediacy of the allene–amine derivative **11** followed by a subsequent rearrangement. As will shown later, this latter pathway was found to be nonproductive in terms of allyl formation; in other words, the k_4 step does not occur.

The results of labeling studies were as follows: for the reaction using $^{13}CH_3I$ the resultant allyl–iodide **8** is labeled at both of the terminal carbons equally, that is, 50% ^{13}C at each position as shown by $^{13}C\{^1H\}$ NMR spectroscopy; similarly, with CD_3I, the product is $Ir(\eta^3\text{-}C_3H_2D_3)I[N(SiMe_2CH_2PPh_2)_2]$ with one deuterium at the central carbon and the remaining two equally distributed at the allyl termini. Since the k_2 step in Scheme IV is the only productive pathway for the formation of the allyl product **8**, this implies that there is another unobserved intermediate(s) formed during the transformation of the isopropenyl complex **10** to **8** which allows scrambling of the label to both ends of the allyl ligand. One possible intermediate is the unobserved allene–hydride derivative **12**, which could form via β-elimination from **10**; as shown in Scheme VI, rotation of the coordinated allene to generate **12′** followed by hydride migratory insertion would product the allyl complex **8**, but only labeled at one end. To scramble the label to both ends requires the allene ligand in **12′** to shift double bonds to generate **12″**, which after allene rotation to form **12‴** and hydride insertion provides for **8** with both ends equally labeled. Alternatively,

Scheme VI

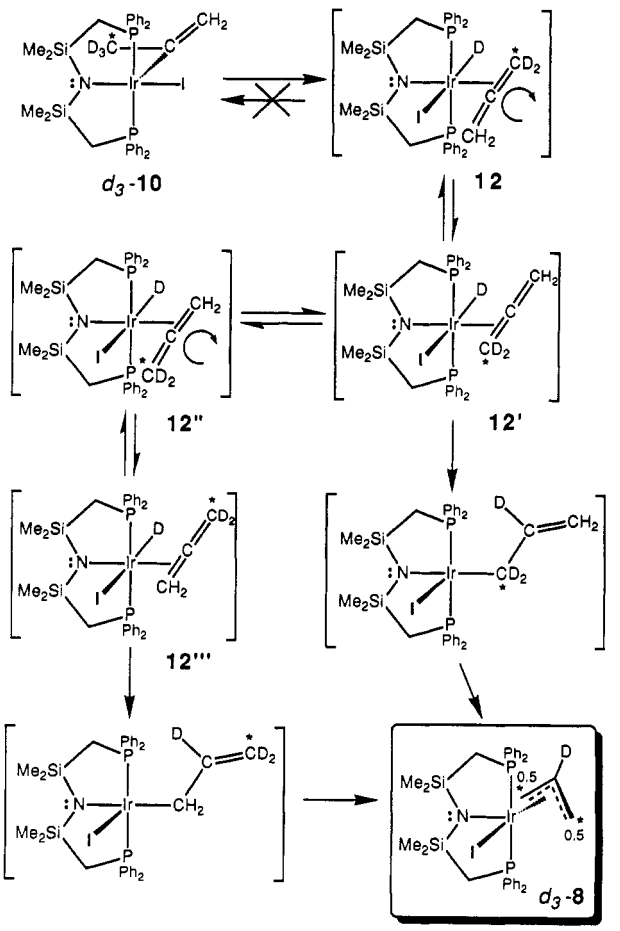

Scheme VII

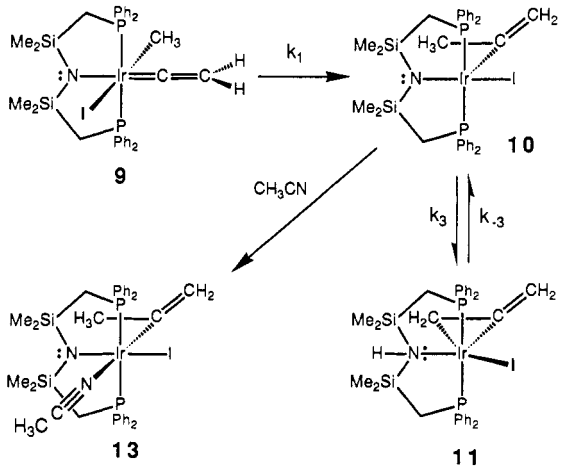

scrambling may occur after the formation of the C–H bond, possibly via a transient η^1-allyl species which undergoes facile σ–π rearrangements before it forms the nonfluxional final product **8**.

Although the details of kinetic studies will be reported separately, one further important aspect is the possibility of reversible steps in the mechanism presented in Scheme IV. For the k_1 step, the migratory insertion of the methyl and vinylidene units, it is unlikely that it is reversible, since there is no literature precedent for such a C–C bond-breaking back-reaction in an acyclic system. The β-proton abstraction from the isopropenyl unit in **10** to form the allene–amine **11**, the k_3 step, is reversible. This was established by a separate experiment in which acetonitrile (3–4 equiv) was added to a mixture containing **9**, **10**, and

(39) Schwartz, J.; Hart, D. W.; McGiffert, B. *J. Am. Chem. Soc.* **1974**, *96*, 5613.
(40) Wolf, J.; Werner, H. *Organometallics* **1987**, *6*, 1164.
(41) Merola, J. S. *Organometallics* **1989**, *8*, 2975–2977.

Scheme VIII

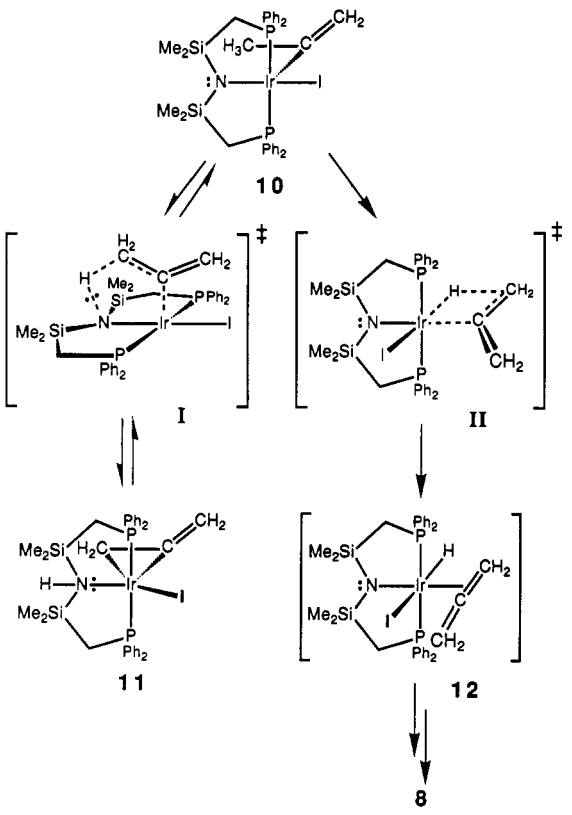

11; analysis by $^{31}P\{^1H\}$ NMR spectroscopy showed that the resonance due to the isopropenyl complex **10** was replaced by the new species **13**, which was characterized as the acetonitrile adduct of **10**, $IrNCCH_3(CMe{=}CH_2)I[N(SiMe_2CH_2PPh_2)_2]$. Further monitoring of this reaction showed that both **9** and the allene–amine derivative **11** rearranged to give the acetonitrile adduct **13** exclusively without formation of the allyl product **8** (Scheme VII). Since acetonitrile traps the five-coordinate complex **10** in a fast step, the observed slow rearrangement of **11** to **13** requires that **10** and **11** be in equilibrium. The fact that the allyl complex did not form under these conditions is strong evidence that it is generated exclusively via the k_2 step in Scheme IV and not via the allene–amine derivative **11**; in other words, the k_4 step is nonproductive. This k_2 step in Scheme IV (representing however many elementary reactions) also cannot be reversible, since this would scramble the label in the isopropenyl complex **10** from the methyl substituent to the β-vinyl position, and this is not observed.

One final point on the mechanism shown in Scheme IV concerns the likely transition states that lead to the various species observed. The reversible transformation of the isopropenyl intermediate **10** to the allene–amine derivative **11** suggests that the apical isopropenyl fragment is deprotonated by the cis-disposed amide lone pair of electrons via a transition state similar to I, shown in Scheme VIII. However, to ultimately form the allyl complex **8**, access to the allene–hydride intermediate **12** has been proposed and this requires a different transition state; one possibility is that the five-coordinate complex **10** rearranges to place the isopropenyl unit trans to the amide donor such that a β-elimination to the iridium center via transition state II in Scheme VIII occurs.

Attempts to extend this carbon–carbon bond-coupling reaction by the addition of other alkyl halides was only partly successful. For example, the addition of ethyl iodide (CH_3CH_2I) to the vinylidne **2** resulted in a series of reactions and color changes similar to that found for the methyl iodide reaction. However, no clean (1-methylallyl)iridium complexes could be isolated, although a number of the analogous intermediates could be detected by ^1H NMR spectroscopy. For example, monitoring the reaction of CH_3CH_2I with **2** clearly showed the presence of the ethyl–iodide oxidative-addition adduct $Ir{=}C{=}CH_2(Et)I[N(SiMe_2CH_2PPh_2)_2]$ and the next intermediate, the isobutenyl derivative $Ir(CEt{=}CH_2)I[N(SiMe_2CH_2PPh_2)_2]$. These intermediates decayed as a function of time to a generate a complex mixture, from which we could not isolate any products; however, some components of this mixture are hydride-containing derivatives, as evidenced by the presence of peaks upfield (from −6 to −25 ppm). To check if the reason for the mixture of products was due to the possibility of isomers of the presumed methylallyl product $Ir(\eta^3\text{-}C_3H_4Me)I[N(SiMe_2CH_2PPh_2)_2]$, the methylallyl–*bromide* complex was prepared via oxidative addition of crotyl bromide (mixture of geometric isomers) to the iridium(I) cyclooctene complex **3**; a single stereoisomeric product was obtained in essentially quantitative yield, and it was determined to be the isomer having the methyl group syn-disposed as shown for **14**. Since there would

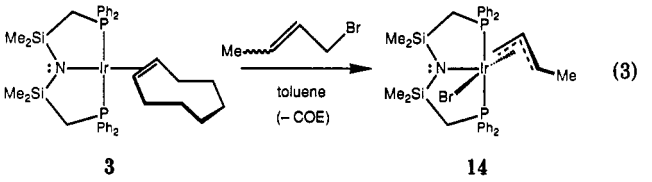

(3)

appear to be nothing untoward about the product, it must be that one of the last steps before formation of the product, perhaps the β-elimination reaction to form the presumed 1-methylallene–hydride derivative or perhaps the nonproductive β-proton abstraction step leading to an unstable substituted allene–amine derivative, is the cause of the mixture of products. The addition of benzyl bromide ($PhCH_2Br$) to the vinylidene complex also resulted in a complex mixture of products.

One final item on the methyl iodide reaction is the curious reaction of the vinylidene complex **2** with *excess* CH_3I. In this case another product can be isolated and was found to be the methyl–diiodide derivative $IrI_2Me[HN(SiMe_2CH_2PPh_2)_2]$ (**15** in eq 4). The ^1H NMR

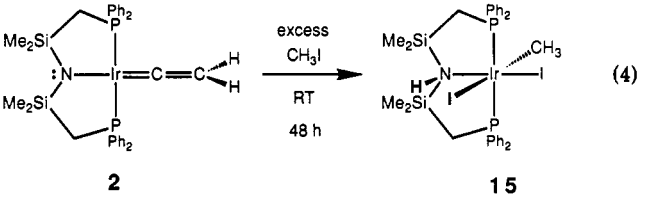

(4)

spectrum of **15** consists of a triplet at 1.35 ppm for $Ir{-}CH_3$ and a resonance at 3.80 ppm for the amine N–H proton. The X-ray crystal structure of **15** has been determined, and full details are reported in the supplementary material. The structure is very similar to those of a series of amine–hydride complexes of iridium and rhodium formed by H_2 addition to methyl–halide precursors.[30] The formation of **15** requires that the vinylidene unit be lost in some manner; when this reaction was monitored by ^1H NMR spectroscopy, allene was detected. Therefore, it is suggested that the amine–diiodide complex **15** is produced via the mechanism shown in Scheme IV with one difference: after β-proton abstraction to generate the allene–amine complex **11**, the excess CH_3I displaces allene and a further oxidative addition occurs to generate **15**. That the parent allene–amine complex **11** is labile to excess CH_3I

does help to rationalize the above-mentioned failures for the CH_3CH_2I and $PhCH_2Br$ reactions with the vinylidene, since these reactions must proceed through substituted-allene intermediates that are potentially even more labile. The formation of **15** can be completely suppressed by adding 2–5 equiv of CH_3I to the vinylidene starting material **2** followed by removal of the excess CH_3I after the formation of the first intermediate **9**.

Conclusions

The results of this study demonstrate that the vinylidene unit can undergo migratory insertion reactions under suitable conditions to generate new carbon–carbon bonds. Oxidative addition of trialkyl derivatives of group 13 to the iridium(I) vinylidene complex **2** has been found to be one method of generating an unobserved species containing an iridium–carbon bond, which can then undergo migratory insertion with the coordinated vinylidene unit to generate an isopropenyl ligand. A notable structural feature found in the solid-state structures of these particular derivatives $Ir(EMe_2)CMe{=}CH_2[N(SiMe_2CH_2PPh_2)_2]$ (E = Al, Ga) is the presence of an iridium–aluminum (iridium–gallium) bond bridged by the amide donor of the ancillary tridentate ligand. Interestingly, other more electron-rich Ir(I) complexes such as $IrMe(PMe_3)_4$ do not form oxidative-addition adducts with AlR_3 species, although adducts of InR_3 can be isolated.[33] Thus, it would appear that the amide donor facilitates this oxidative addition by stabilization of the AlR_2 (and $GaMe_2$) part of the addend.

A classic way to generate an iridium–carbon bond is via oxidative addition of simple alkyl halides to a suitable iridium(I) precursor.[35] For the case of CH_3I, its reaction with the vinylidene complex ultimately leads to the formation of the iridium(III) alkyl derivative $Ir(\eta^3\text{-}C_3H_5)I[N(SiMe_2CH_2PPh_2)_2]$. This process also involves migratory insertion of a vinylidene unit into the iridium–carbon bond, as evidenced by spectroscopic monitoring of the reaction in which a number of intermediates could be observed and characterized. In fact, we have been able to observe for the first time the vinylidene–alkyl species and follow the actual migratory insertion step. Previous workers have only been able to postulate this as an intermediate step based on product analysis and labeling studies.[10,20,21]

The ability of a vinylidene unit to undergo migratory insertion reactions is reminiscent of the migratory insertion behavior of coordinated carbon monoxide. There is an analogy here between a carbonyl ligand and a vinylidene ligand (and extends to alkylidene/carbene type ligands as well) which merits some discussion. It is known that there is an equilibrium between a carbonyl–hydrocarbyl complex and an acyl species, i.e., $MR(CO) \rightleftarrows MCOR$; indeed, in certain cases this equilibrium can be shifted in either direction by addition/loss of ligand. However, there is no similar equilibrium known for a vinylidene–hydrocarbyl complex. In other words, the "deinsertion" step, the formation of a vinylidene–hydrocarbyl species from a substituted alkenyl derivative, requires that a carbon–carbon bond be broken, and this would appear to be thermodynamically uphill unless ring stain is being relieved.[42,43]

The transformation of an isopropenyl moiety to an allyl fragment requires a 1,2-metal-for-hydrogen shift, as shown schematically in eq 5. It has been suggested[39–41] that such

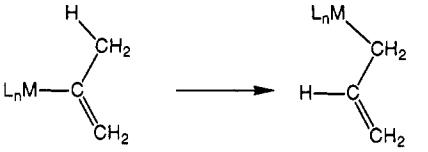

(5)

a rearrangement occurs via a β-elimination step to generate an as yet unobserved allene–hydride intermediate, which then undergoes hydride transfer to the central carbon of the allene ligand to form the coordinated allyl moiety. As shown in this work, this rearrangement is a likely pathway for the production of the allyl–iodide complex **8**. However, there is a parallel, nonproductive sequence that apparently involves an initial proton transfer from the methyl substituent to the coordinated amide donor to form the allene–amine complex **11**. Such a process whereby proton transfer is competitive between a metal and a ligand is intriguing and may be quite general when basic ligands are present in the coordination sphere.[44]

Acknowledgment. The NSERC of Canada is gratefully acknowledged for financial support. We also thank Johnson Matthey for the loan of $IrCl_3$.

Supplementary Material Available: Tables of hydrogen atom coordinates, anisotropic thermal parameters, bond lengths, bond angles, torsion or conformation angles, intermolecular distances involving both the non-hydrogen atoms and the hydrogen atoms, and least-squares planes for $Ir{=}C{=}CH_2[N(SiMe_2CH_2PPh_2)_2]\cdot C_6H_5CH_3$, $Ir(AlMe_2)CMe{=}CH_2[N(SiMe_2CH_2PPh_2)_2]$, $Ir(GaMe_2)CMe{=}CH_2[N(SiMe_2CH_2PPh_2)_2]$, $Ir(\eta^3\text{-}C_3H_5)I[N(SiMe_2CH_2PPh_2)_2]$, and $IrMeI_2[HN(SiMe_2CH_2PPh_2)_2]\cdot C_6H_6$ (87 pages). Ordering information is given on any current masthead page.

OM920159N

(42) Stenstrom, Y.; Jones, W. M. *Organometallics* **1986**, *5*, 178.
(43) Stenstrom, Y.; Klauck, G.; Koziol, A.; Palenik, G.; Jones, W. M. *Organometallics* **1986**, *5*, 2155.
(44) Fryzuk, M. D.; Bhangu, K. *J. Am. Chem. Soc.* **1988**, *110*, 961.